

# UC San Diego

## UC San Diego Electronic Theses and Dissertations

### Title

Activity of Energy Metabolic Enzymes in Different Coral Species and Populations Provides Evidence for Local Adaptation

### Permalink

<https://escholarship.org/uc/item/7n98c9vk>

### Author

Hassibi, Cameron Makan

### Publication Date

2020

Peer reviewed|Thesis/dissertation

UNIVERSITY OF CALIFORNIA SAN DIEGO

Activity of Energy Metabolic Enzymes in Different Coral Species and Populations  
Provides Evidence for Local Adaptation

A Thesis submitted in partial satisfaction of the requirements  
for the degree Master of Science

in

Marine Biology

by

Cameron Makan Hassibi

Committee in Charge:

Professor Martin Tresguerres, Chair  
Professor Ronald Burton  
Professor Jennifer Taylor

2020

Copyright

Cameron Makan Hassibi, 2020

All rights reserved.

The Thesis of Cameron Makan Hassibi is approved, and it is acceptable in quality and form for publication on microfilm and electronically:

---

---

---

Chair

University of California San Diego

2020

## DEDICATION

For my mother, Mitra Ghadimi, who taught me strength, and for my father, Mohammad Hassibi,  
who taught me compassion.

## EPIGRAPH

“Yes, as everyone knows, meditation and water are wedded for ever.”  
-Herman Melville

## TABLE OF CONTENTS

Signature Page .....	iii
Dedication .....	iv
Epigraph .....	v
Table of Contents .....	vi
List of Abbreviations .....	vii
List of Figures .....	viii
List of Tables .....	x
Acknowledgements .....	xi
Abstract of the Thesis .....	xii
Introduction .....	1
Materials & Methods .....	14
Results .....	19
Discussion .....	24
Appendix .....	32
References .....	42

## LIST OF ABBREVIATIONS

<b>ATP</b>	Adenosine triphosphate
<b>NADH</b>	Nicotinamide adenine dinucleotide
<b>Acetyl-CoA</b>	Acetyl coenzyme A
<b>TCA</b>	Tricarboxylic acid cycle
<b>CS</b>	Citrate synthase
<b>MDH</b>	Malate dehydrogenase
<b>FADH<sub>2</sub></b>	Flavin adenine dinucleotide
<b>H<sup>+</sup></b>	Hydrogen ion
<b>ADP</b>	Adenosine diphosphate
<b>Pi</b>	Phosphate ion
<b>LDH</b>	Lactate dehydrogenase
<b>OpDH</b>	Opine dehydrogenase
<b>SDH</b>	Strombine dehydrogenase
<b>ADH</b>	Alanopine dehydrogenase
<b>cMDH</b>	Cytoplasmic malate dehydrogenase
<b>mMDH</b>	mitochondrial malate dehydrogenase
<b>PAR</b>	Photosynthetically active radiation
<b>RCF</b>	Relative centrifugal force
<b>BSA</b>	Bovine serum albumin
<b>SEM</b>	Standard error of the mean
<b>UVR</b>	Ultraviolet radiation



## LIST OF FIGURES

Figure 1: Edited from Hochacka and Somero (2002). Compilation diagram of the main processes involved in ATP production under aerobic and anaerobic conditions.....	8
Figure 2: Bocas del Toro experimental locations are shown along with the location of the Smithsonian Tropical Research Institute (STRI) station.....	11
Figure 3: Enzymatic activity of malate dehydrogenase (MDH), lactate dehydrogenase (LDH), strombine dehydrogenase (SDH), alanopine dehydrogenase (ADH), and citrate synthase (CS) for <i>A. cervicornis</i> .....	21
Figure 4: Enzymatic activity of malate dehydrogenase (MDH), lactate dehydrogenase (LDH), strombine dehydrogenase (SDH), alanopine dehydrogenase (ADH), and citrate synthase (CS) for <i>P. astreoides</i> .....	22
Figure 5a: <i>A. cervicornis</i> MDH: Graphical representations of the results as reported in Figure 3 presented alongside their corresponding two-way ANOVA tables. Tabular results of Tukey’s multiple comparisons tests are also provided where significant effects were detected .....	32
Figure 5b: <i>A. cervicornis</i> LDH: Graphical representations of the results as reported in Figure 3 presented alongside their corresponding two-way ANOVA tables .....	33
Figure 5c: <i>A. cervicornis</i> SDH: Graphical representations of the results as reported in Figure 3 presented alongside their corresponding two-way ANOVA tables .....	34
Figure 5d: <i>A. cervicornis</i> ADH: Graphical representations of the results as reported in Figure 3 presented alongside their corresponding two-way ANOVA tables. Tabular results of Tukey’s multiple comparisons tests are also provided where significant effects were detected .....	35
Figure 5e: <i>A. cervicornis</i> CS: Graphical representations of the results as reported in Figure 3 presented alongside their corresponding two-way ANOVA tables .....	36
Figure 6a: <i>P. astreoides</i> MDH: Graphical representations of the results as reported in Figure 4 presented alongside their corresponding two-way ANOVA tables. Tabular results of Tukey’s multiple comparisons tests are also provided where significant effects were detected .....	37
Figure 6b: <i>P. astreoides</i> LDH: Graphical representations of the results as reported in Figure 4 presented alongside their corresponding two-way ANOVA tables .....	38
Figure 6c: <i>P. astreoides</i> SDH: Graphical representations of the results as reported in Figure 4 presented alongside their corresponding two-way ANOVA tables. Tabular results of Tukey’s multiple comparisons tests are also provided where significant effects were	

detected .....	39
Figure 6d: <i>P. astreoides</i> ADH: Graphical representations of the results as reported in Figure 4 presented alongside their corresponding two-way ANOVA tables. Tabular results of Tukey’s multiple comparisons tests are also provided where significant effects were detected .....	40
Figure 6e: <i>P. astreoides</i> CS: Graphical representations of the results as reported in Figure 4 presented alongside their corresponding two-way ANOVA tables. Tabular results of Tukey’s multiple comparisons tests are also provided where significant effects were detected .....	41

## LIST OF TABLES

Table 1: Ratios of fermentative to aerobic metabolic capacity for <i>A. cervicornis</i> and <i>P. astreoides</i> . Smaller LDH+SDH+ADH:CS ratio values are representative of higher aerobic enzyme activity relative to that of fermentative activity and vice versa.....	23
---	----

## ACKNOWLEDGEMENTS

I would like to acknowledge and thank several key figures in their support of my scientific endeavors and, ultimately, the materialization of this thesis.

Martin Tresguerres, principle investigator and the chair of my thesis committee, provided constant encouragement and sage advice in the laboratory and beyond—without whom I would not be the scientist I am today. It was with his compassion and understanding that I was able to complete my greatest achievement for which I am eternally grateful.

My mentor, Lauren Linsmayer, who took me under her wing in preparation for my own research. Despite only working together for one summer, the knowledge and insight I gained under her tutelage aided me inestimably. I would not be where I am today if it were not for her.

Ron Burton and Jennifer Taylor, participating members of my thesis committee, inspired me early on as I navigated my undergraduate career. Their patience and flexibility, although thoroughly tested, was unfaltering.

David I. Kline, experienced coral harvester and resident field expert, helped save me a trip to Bocas del Toro, Panama by working alongside Martin Tresguerres to collect the various coral samples analyzed in this study. Their complimentary expertise and hard work as co-principle investigators facilitated the generation of novel research into coral cellular physiology which will undoubtedly continue to proliferate in the coming years.

Funding for this study was awarded to David I. Kline and Martin Tresguerres by the National Science Foundation, Division of Ocean Sciences #1538495: “Cellular physiological mechanisms for coral calcification and photosynthesis: extending lab-based models to the field.” This Thesis is coauthored with Hassibi, Cameron M., Tresguerres, Martin, and Kline, David I. The thesis author was the principle researcher/author of the Thesis.

## ABSTRACT OF THE THESIS

Activity of Energy Metabolic Enzymes in Different Coral Species and Populations  
Provides Evidence for Local Adaptation

by

Cameron Makan Hassibi

Master of Science in Marine Biology

University of California San Diego, 2020

Professor Martin Tresguerres, Chair

Anthropogenic alterations to the Earth system threaten the persistence of coral reef ecosystems, yet pervasive knowledge gaps in basic coral biology prevent accurate measures of coral health prior to mortality. The goal of this thesis is to characterize the metabolic signatures of spatially distinct coral populations adapted to the light regimes of their microenvironments using pathway-specific enzymatic assays. Shallow (3 meters) and deep (5-8 meters) *Acropora cervicornis* and *Porites astreoides* populations were sampled at two distinct reef sites: Punta Caracol—a turbid lagoon habitat with large influxes of terrestrial sediments—and Eric Reef—a comparatively pristine open-ocean habitat characterized by greater water column clarity. Coral tissues collected from Bocas del Toro, Panama were homogenized and prepared for analysis at

Scripps Institution of Oceanography (San Diego). Malate dehydrogenase (MDH), lactate dehydrogenase (LDH), strombine dehydrogenase (SDH), alanopine dehydrogenase (ADH), and citrate synthase (CS) enzymatic assays were employed to represent maximum fermentative and aerobic metabolic capacities by measuring changes in peak absorbance readings via spectrophotometry. Maximum changes in absorbance were standardized against actual protein concentrations in a novel methodology developed for this thesis. Calculated maximum enzymatic activities indicate that the energy metabolic pathways of *A. cervicornis* and *P. astreoides* are tuned to local environmental conditions that, generally, favor fermentation in Punta Caracol as suggested by the higher activities of the various opine dehydrogenases.

# INTRODUCTION

## **General Introduction**

Well-observed trends in coral reef biology depict patterns of decline in ecosystem biodiversity and function as a result of interacting anthropogenic stressors on local, regional, and global scales<sup>1-4</sup>. Due to the highly productive nature of reef systems<sup>5,6</sup>, their continued degradation is predicted to have extensive ecological and socioeconomic repercussions<sup>5,7-9</sup> which will undoubtedly increase in the absence of drastic and consequential measures<sup>10</sup>. Despite the seemingly vast amount of resources allocated to research and conservation efforts thus far, there remains a strong consensus among experts that more needs to be done to ensure the persistence of coral reefs<sup>11</sup>. This demands the urgent burgeoning of scientific inquiries to identify and close pervasive knowledge gaps in basic coral biology<sup>12,13</sup>. These gaps have the potential to severely hamper the efficacy of future policy measures intended to promote reef vitality<sup>14</sup>. Even relatively straightforward management strategies such as the redistribution of resources to reduce the mismatch between regions of high reef biodiversity and low conservation success rates would likely prove futile without robust and definitive datasets that correctly identify these gaps<sup>10,11,15</sup>.

Although the prospect of tackling the myriad of unknowns plaguing coral research is undoubtedly daunting, such is the task necessary to limit future declines in reef structure, function, and resiliency. Given that the combined negative effect of multiple anthropogenic stressors including sedimentation, coastal development, pollution, overfishing, rising sea surface temperatures, and ocean acidification is far greater in magnitude than the sum of its parts, preserving existing reef system configurations is increasingly unlikely<sup>16</sup>. Instead, efforts must be properly reallocated across multiple disciplines to mitigate the inevitable shifts in coral reef

communities worldwide. An integral component of this multifaceted strategy involves improving our understanding of corals at the cellular and molecular level and their downstream physiological processes that drive coral stress responses—the mechanisms of which remain largely unstudied<sup>17,18</sup>. But while such efforts have gained significant recognition in recent years<sup>19–21</sup>, the integration between coral cell physiology with field work is still required . Applying such integrative procedures in the framework of coral metabolism may help elucidate the fine-scale signatures characterizing coral acclimation strategies, which may prove vital for monitoring changes in coral health prior to mortality<sup>22</sup>. With this in mind, my thesis studied molecular parameters involved in coral energy metabolism, which is intrinsically linked to physiological health and status<sup>23,24</sup>. Enzyme kinetic assays were utilized here to quantify metabolic capacity in the context of local adaptation by examining depth- and location-specific populations of the Caribbean corals *Acropora cervicornis* and *Porites astreoides*. This approach may greatly enhance our ability to proactively recognize and neutralize anthropogenic threats to coral reef systems on sufficiently-truncated timescales—thereby circumventing irreversible habitat deterioration that may otherwise occur without timely and targeted intervention<sup>19</sup>.

### **General coral biology and symbiotic association**

Corals are members of the phylum Cnidaria, class Anthozoa. Different coral species are scattered across a broad range of habitats and niches, which reflects their complex life histories forged via adaptive responses to changing environmental conditions, disturbances, and stressors over hundreds of millions of years<sup>25–27</sup>. Despite this diversity, most of our current knowledge pertains to reef-building corals (Scleractinia) found throughout the oligotrophic shallows of the low-latitude oceans<sup>28</sup>—due in large part to the importance of these ecosystems to human populations<sup>29</sup>. Through tightly regulated and highly integrated metabolic processes<sup>30</sup>, these



underwater architects deposit calcium carbonate skeletons which form the massive three-dimensional reef structures that dominate the endemic seascape. As is the case with all cnidarians, corals are diploblastic organisms with two distinct germ layers: the ectoderm and the endoderm (also referred to as ‘gastrodermis’ in the literature). These tissues interfold to form a shared gastrovascular compartment known as the coelenteron. This fluid-filled cavity permits, among other functions, the transport and exchange of metabolic intermediates, waste products, endosymbiotic algae (discussed at length below and in subsequent sections), and nutrients throughout the colony. Surrounding either side of the coelenteron is an ectodermal and endodermal cell layer. Layers adjacent to the surrounding seawater are the oral ectoderm and oral endoderm while those enveloping the coral skeleton are the aboral endoderm and aboral ectoderm.

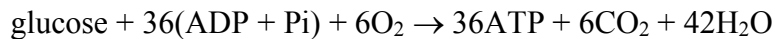
Coral colonies are comprised of genetically identical polyps interconnected by means of the coelenteron and the skin-like coenosarc that covers its outermost surface. Surrounded by feeding tentacles, mouths situated at the center of each polyp regulate contact between the chemically distinct fluid of the coelenteron and the surrounding seawater. The polyp mouths are also the point of initial acquisition and final expulsion of *Symbiodinium*, with which they form an intracellular symbiotic association. Along with the complex assemblages of microbes— analogous to that of the human gut microbiome—these photosynthetic endosymbionts form unique partnerships with their coral hosts in what is often cited as the coral holobiont<sup>21</sup>. Although such mutualistic relationships are not uncommon in marine invertebrates, the coral-*Symbiodinium* holobiont is unique in its role as an ecosystem engineer whose presence profoundly influences the structural characteristics of dependent communities<sup>31,32</sup>. The exchange of metabolites and nutrients is one of the defining features of the coral-dinoflagellate symbiosis

and elucidates the persistence of tropical reefs in traditionally nutrient-replete environments. Algae-derived fixed carbon generated via photosynthesis is translocated from the symbiont to the coral host for use in mucus generation, respiration, growth, and reproduction<sup>33</sup>. Furthermore, the oxygen waste generated by this same process may promote aerobic metabolism and calcification rates in the coral host<sup>34</sup>. In return, corals provide their endosymbionts with protection and nutrients in the form of host metabolic waste products<sup>16,33</sup>.

### **General aerobic and fermentative metabolism**

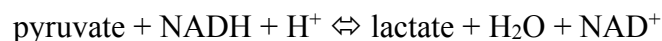
Key to the survival of all life is the balance between energy consumption and generation. Adenosine triphosphate (ATP) is the universal currency in this exchange and is produced via three basic pathways: phosphagen mobilization, fermentation, and oxidative metabolism<sup>35</sup>. These ATP-synthesizing mechanisms are categorized as either aerobic (oxygen-dependent) or anaerobic (oxygen-independent) metabolic processes. Phosphagen mobilization is the simplest of these pathways and is most closely associated with burst muscular work<sup>36</sup>. The mobilization of phosphagens is modulated by creatine phosphokinase and does not require oxygen. Fermentation is also oxygen-independent and involves the partial catabolism of substrates to various anaerobic end-products—with anaerobic glycolysis being the most prevalent and well-conserved of the fermentative processes<sup>35</sup>. Anaerobic glycolysis is a fermentative pathway by which a six-carbon glucose molecule is converted into two three-carbon pyruvate molecules through a series of enzyme-catalyzed reactions<sup>37</sup>. Comprised of an energy investment phase and an energy production phase, the glycolytic pathway provides multiple access points for regulatory agents to intervene as dictated by the energy demands of the cell. The production of pyruvate from glucose yields two molecules of ATP, two molecules of nicotinamide adenine dinucleotide (NADH), and two molecules of pyruvate.

During aerobic conditions, adequate cellular oxygen concentrations favor the more efficient and complete oxidation of pyruvate. The pyruvate provided by the glycolytic pathway is transported into the mitochondria where it is oxidized by the pyruvate dehydrogenase complex into acetyl coenzyme A (acetyl-CoA)—the starting material for the citric acid cycle or tricarboxylic acid (TCA) cycle. As is the case with anaerobic glycolysis, the TCA cycle may be modulated at various phases through complex molecular interactions. The TCA cycle, in relative terms, begins with the condensation of acetyl-CoA and oxaloacetate by the enzyme citrate synthase (CS) to form citrate and ends with the formation of oxaloacetate from malate via malate dehydrogenase (MDH). In a single turn of the cycle, only one molecule of ATP is generated. The true measure of energy generation, however, lies in the three molecules of NADH (four when including the NADH produced from pyruvate dehydrogenase) and the one molecule of flavin adenine dinucleotide (FADH<sub>2</sub>) formed alongside the single ATP molecule. These cofactors provide the electrons utilized in the electron transport system of the inner mitochondrial membrane where the bulk of ATP is generated. In addition to the glycolytic pool of cytoplasmic NADH, the various cofactors produced by the TCA cycle are stripped of their electrons by a series of complexes that form the respiratory chain involved in oxidative phosphorylation. The transport of electrons through the various inner membrane-bound protein complexes fuels the pumping of hydrogen ions (H<sup>+</sup>) out of the mitochondrial matrix and into the intermembrane space. The creation of a H<sup>+</sup> concentration gradient permits the downhill movement of protons back into the mitochondrial matrix. This proton leak provides the driving force for ATP synthesis from adenosine diphosphate (ADP) and phosphate ions (Pi)—a thermodynamically unfavorable reaction catalyzed by the inner mitochondrial membrane-bound ATP synthase enzyme. The net reaction for the complete oxidation of glucose is as follows:



The complete aerobic oxidation of 1 mole of glucose yields an estimated 36-38 moles of ATP—drastically greater than that of fermentative glycolysis (Figure 1)<sup>38</sup>.

However, during oxygen limitation leading to anaerobic conditions, mitochondrial pyruvate oxidation is inhibited. Consequentially, the reoxidation of NADH to NAD<sup>+</sup> that would normally occur aerobically must do so in the absence of oxygen. It is the role of the terminal dehydrogenase enzyme to then facilitate the reductive condensation of pyruvate coupled to NAD<sup>+</sup> regeneration. In vertebrate animals and some invertebrates experiencing oxygen limitation, the pyruvate formed via glycolysis is not shuttled into mitochondria and instead is converted to lactate by lactate dehydrogenase (LDH) in the cytoplasm<sup>22</sup>. This reaction regenerates the NAD<sup>+</sup> co-factor necessary to facilitate a continuous flux of glycolysis for ATP production during periods of oxygen-limitation<sup>39,40</sup>:



LDH

However, some invertebrates, rely upon alternative terminal pyruvate dehydrogenases known as “opine dehydrogenases” (OpDHs). The functional role of opine dehydrogenases is the same as LDH. (i.e. to regenerate NAD<sup>+</sup>) However unlike LDH, these OpDHs) require an additional substrate in the form of an amino acid to catalyze the reductive condensation of pyruvate, yielding an imino acid (or opine) end-product<sup>41-43</sup> as illustrated below:



### OpDH

Possible advantages of OpDH use over the LDH equivalent include higher yields of ATP, maintenance of constant intracellular osmotic pressure, lower NADH/NAD<sup>+</sup> ratios, and reduced acidosis<sup>35,44,45</sup>.

Further illustrating the exemplary adaptive capacity of this oxygen-independent metabolic pathway is the presence of the diverse and functionally analogous OpDHs in many marine invertebrate species and tissues<sup>35,46</sup>. These OpDHs include strombine dehydrogenase (SDH) and alanopine dehydrogenase (ADH) among others, and function similarly to LDH in maintaining the proper NADH/NAD<sup>+</sup> balance to drive anaerobic glycolysis<sup>47</sup>. The switch from aerobic to fermentative metabolism provides organisms with an rapid means of energy genesis at the expense of efficiency<sup>48,49</sup> and is, therefore, considered generally unsustainable over extended periods of time<sup>40</sup>. Nonetheless, the flexibility inherent in glycolytic fermentation grants a key evolutionary advantage to marine invertebrates and helps explain its wide phylogenetic conservation<sup>50</sup>.

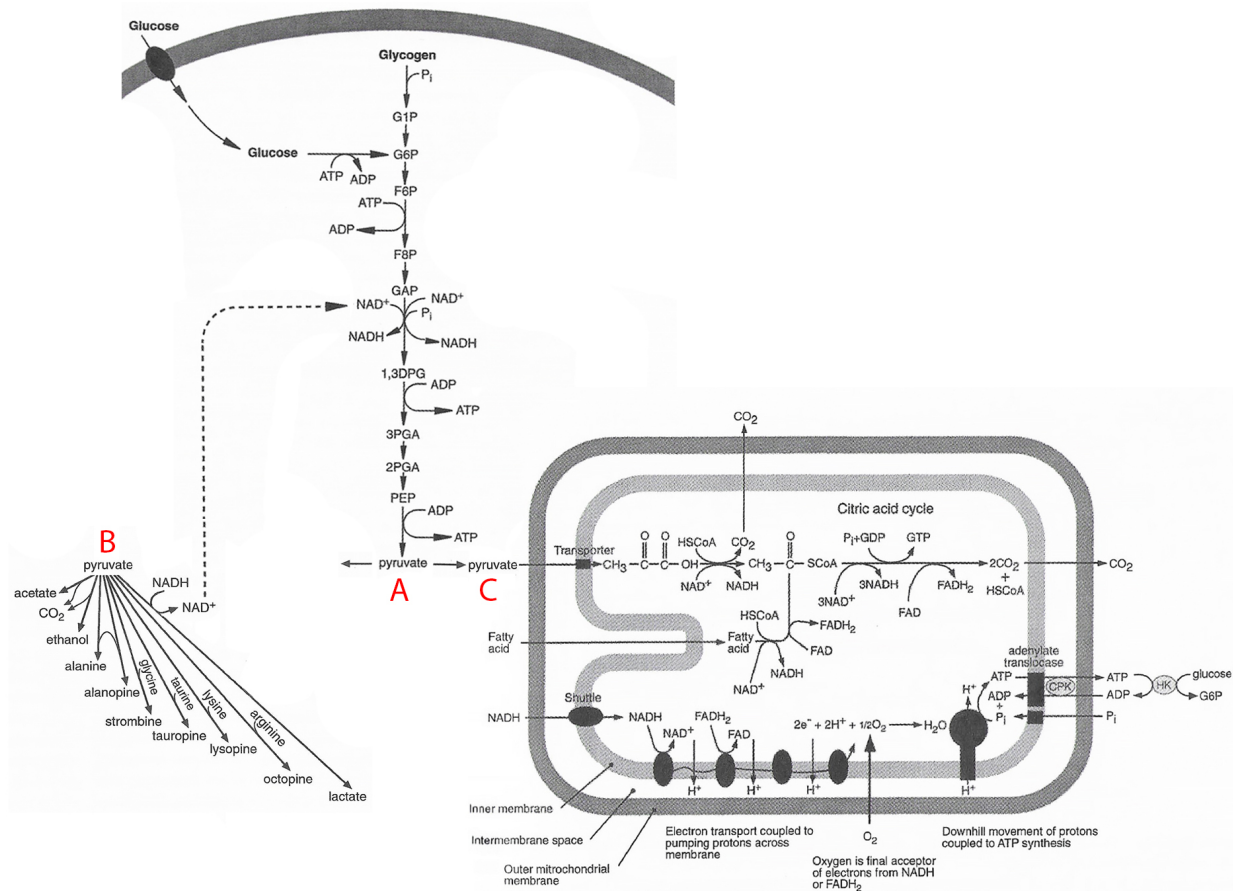


**Figure 1:** Edited from Hochacka and Somero (2002). Compilation diagram of the main processes involved in ATP production under aerobic and anaerobic conditions. Under anaerobic conditions, (A) pyruvate generated via glycolysis is fermented (B) to regenerate NAD<sup>+</sup> necessary to drive glycolysis. In addition to NAD<sup>+</sup>, the fermentation of pyruvate via dehydrogenase enzyme produces an imino acid end product—all of which are functionally analogous. Under aerobic conditions, (C) pyruvate is transported to the mitochondria to generate ATP via oxidative metabolism.

## Coral metabolic biochemistry

At daytime, photosynthesis by coral symbiotic algae provides an ample supply of oxygen that can sustain aerobic metabolism<sup>33</sup>. However, at night, respiration by the coral holobiont can deplete oxygen levels leading to hypoxia and increased reliance on fermentative pathways to produce ATP<sup>51</sup>. Additionally, shifts in the use of aerobic and fermentative energy metabolic pathways can potentially also occur during exposure of other environmental conditions that affect oxygen and fuel supply; in particular depth and water turbidity (which affect

photosynthesis), water flow, and prey availability. However, coral fermentative pathways and the regulation of energy metabolism during aerobic and anaerobic conditions are surprisingly poorly characterized. On the other hand, the fine-tuning of aerobic and fermentative pathway utilization is a well-documented phenomenon in marine intertidal invertebrates<sup>47</sup>, and can provide cues to about some of the potential strategies utilized by coral. Intertidal invertebrates experience regular bouts of environmental and functional hypoxia and anoxia<sup>52</sup> at which time the generation of ATP via aerobic metabolism is impaired and a compensatory shift to glycolytic fermentation is observed<sup>35,39,53</sup>.

The existence of these alternative energetic mechanisms in marine invertebrates including corals provides a unique opportunity for the improved characterization of metabolic pathway plasticity in coral populations photoacclimated to their microenvironment. Similar techniques were employed in a recent study to determine metabolic enzyme activities in response to oxygen deprivation in the Hawaiian reef-building coral *Montipora capitata*, in which these enzymes served as proxies for coral hypoxic stress<sup>22</sup>. This thesis sought to expand on the concept by including the analysis of two additional metabolic enzymes, citrate synthase (CS) and malate dehydrogenase (MDH), to better resolve the unknowns persistent in coral adaptive physiological responses. CS is a mitochondrial enzyme that catalyzes the condensation reaction of acetyl-CoA and oxaloacetate to form citrate in the first step of the TCA cycle<sup>48</sup>. Due to its specific role within the mitochondria, CS is the ideal candidate to represent general aerobic capacity<sup>54</sup>. MDH differs from all other enzymes of interest due to its broad involvement in multiple metabolic pathways<sup>55,56</sup>. MDH plays a crucial role in both aerobic and fermentative metabolism as an energy-supplying enzyme<sup>57-59</sup>. The mitochondrial MDH isoenzyme (mMDH), which catalyzes the oxidation of malate in the TCA cycle, and the cytoplasmic MDH isoenzyme (cMDH), which

primarily reduces oxaloacetate in the cytoplasm, function as transporters of reducing equivalents through various shuttle systems<sup>57,60–62</sup>. This coordinated effort between mMDH and cMDH helps regulate the cytoplasmic redox state of a cell by continually shunting NADH generated in the cytoplasm into the mitochondrial matrix for further ATP production via oxidative phosphorylation<sup>46,60,63</sup>. Despite lacking pathway specificity, observations of its maximum activities in coral tissues are nevertheless valuable as supplementary indicators for general metabolic scope.

### **Effect of light on coral metabolism**

In ideal light conditions, photosynthesis contributes the overwhelming majority of organic carbon used by the coral when compared to that of heterotrophy<sup>64</sup>. In addition to supplying fixed carbon to host tissues, photosynthesis generates oxygen as a waste-product which is made available to the coral host. Oxygen is critical in its role as a direct and indirect driver of many physiological processes in corals<sup>65</sup>, and its availability dictates the metabolic pathways utilized by the coral host. As the prerequisite for ATP-synthesis via mitochondrial oxidative phosphorylation, oxygen enables the complete oxidation of glucose via aerobic metabolism<sup>66</sup>. In the absence of adequate oxygen concentrations, cellular metabolism relies on fermentative pathways to generate ATP. The relationship between photosynthesis and oxygen production is therefore dictated primarily by the availability of light energy, wherein photosynthetic activity affects the concentration of oxygen within the host tissue<sup>67,68</sup>. Consequentially, the growth, reproduction, and survival of the coral-algal holobiont is dependent on the spectral irradiance of light available<sup>69</sup>. For the sessile obligate zooxanthellae corals, reliance on a highly variable resource such as light requires adaptive physiological responses to changes in photosynthetically active radiation (PAR). While light has long been observed as a



major limiting factor in the depth-distribution of hermatypic corals<sup>70–72</sup>, the intricacies of local adaptation elucidated by intra-specific and population-based studies continue to illustrate a need for a universal proxy which accurately depicts changes to corals’ aerobic and fermentative capacities prior to mortality. To that end, efforts to bridge the gap between coral bioenergetics and conservation have expanded—as evident by this thesis and in parallel research efforts—and, coincidentally, aligns well with the growing threat of elevated sedimentation and nutrient stress on coral reefs in Bocas del Toro, Panama<sup>73</sup> (Figure 2).

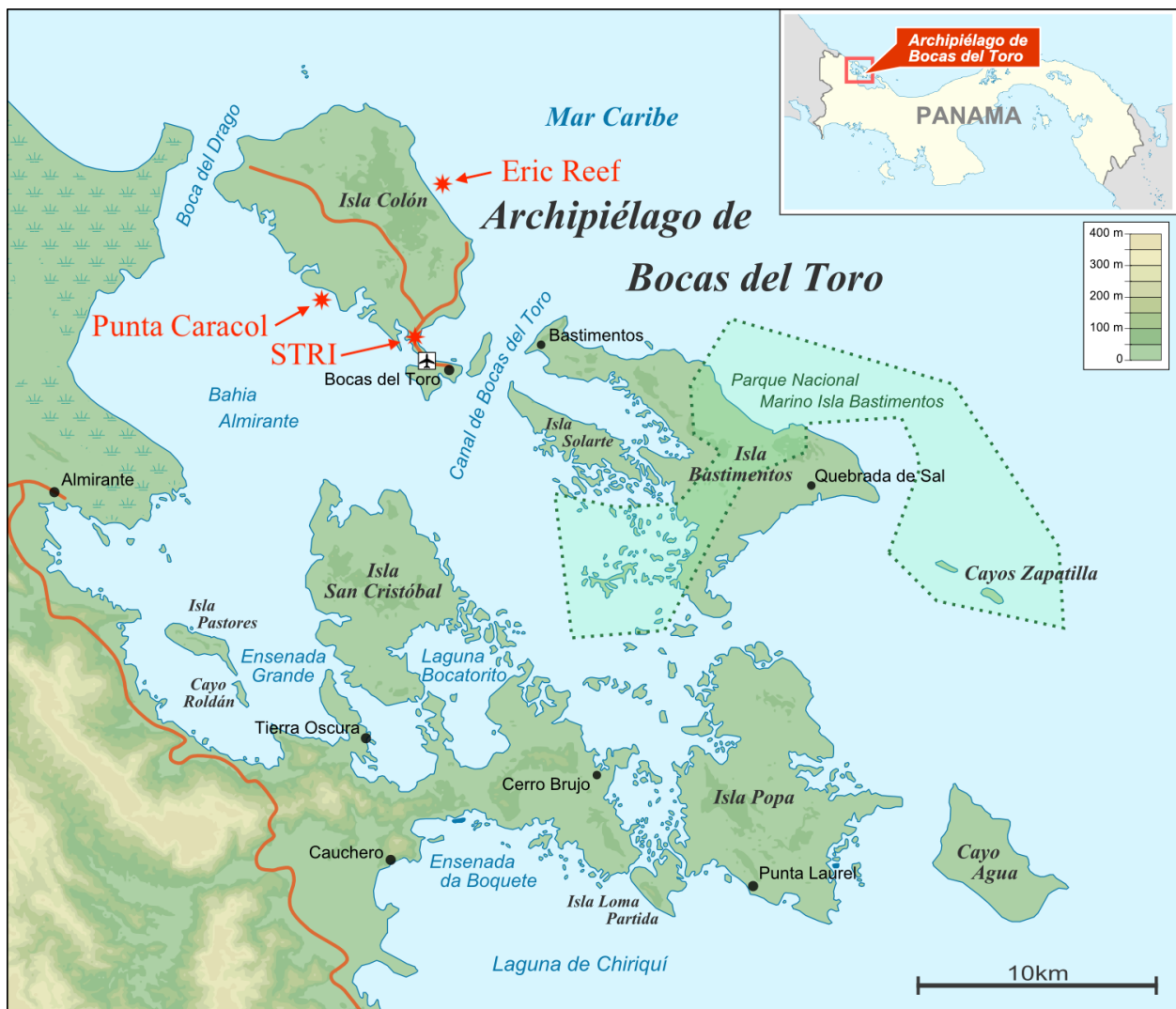


**Figure 2:** Bocas del Toro experimental locations are shown along with the location of the Smithsonian Tropical Research Institute (STRI) station.

Bocas del Toro is a western province in the Republic of Panama spanning an area of 8,917 km<sup>2</sup> along a narrow continental shelf<sup>74</sup>. With a coastal zone reaching maximum depths of 20-50 meters divided between the two large lagoons Bahía Almirante and Laguna de Chiriquí, the collection sites of Punta Caracol and Eric Reef sit on opposite sides of Isla Colón within the north-western portion of Bahía Almirante<sup>75</sup>. Punta Caracol is a mainland-facing reef site within the Bahía Almirante where terrestrial runoff and nutrient pollution—exacerbated by limited ocean flushing—contribute to elevated water turbidity<sup>75</sup>. In contrast, Eric Reef is exposed to the Caribbean Sea and, as a result, experiences less terrestrial influence and higher rates of water exchange with the open ocean. Consequentially, water turbidity is low and diurnal CO<sub>2</sub>/pH ranges more closely resemble that of the open ocean<sup>75,76</sup>.

The marine ecosystems of the Bocas del Toro archipelago are vulnerable due to abundant peak regional rainfall of 287 cm per year and expanding land development, deforestation, and agricultural works within the last decade. As a result, rates of sedimentation, heavy-metal contaminants, and nutrient runoff into these local marine habitats via regional and seasonal rivers has increased<sup>75</sup>. Mangrove forests, which offer protection to neighboring coral reefs from the aforementioned terrestrial inputs, are threatened within both the Bahía Almirante and Laguna de Chiriquí by coastal development and climate change<sup>77</sup>. The combination of enhanced sedimentation and eutrophication, compounded by the continued loss of natural buffer systems like that of mangrove forests, threatens the critical light resource almost all hermatypic corals need to survive<sup>8</sup>.

Suspended particles carried into coastal marine habitats by freshwater sources can alter both the intensity and spectral quality of available light reaching individual corals, thereby impacting their metabolism<sup>78</sup>. Elevated nutrient inputs also support the overgrowth of algae

leading to reduced water transparency. A 5-week shading experiment of *A. cervicornis* at San Cristobal Reef off southwest Puerto Rico notes decreases in net primary productivity and respiration as a function of light exclusion<sup>79</sup>, which reflects the interplay of sufficient solar radiation and water clarity on coral vitality. Similarly, an investigation involving turbidity stress on coral reefs revealed that the energy state of corals is extremely sensitive to anomalies in turbidity and depth<sup>80</sup>. Turbidity-induced light attenuation may manifest in reef structures as a shoaling of coral zonation over sufficient timescales, potentially resulting in short-term losses in deeper coral populations<sup>81</sup>. This phenomenon might be exacerbated in specific colonies that lack the photo- and heterotrophic plasticity required to offset energetic deficiencies during periods of high water column turbidity<sup>82</sup>. Given the potential for future declines in water clarity and PAR penetration, there is a need to further understand the species- and spatial-specific adaptive capabilities of corals to light resource availability. While the number of available studies investigating the photoacclimation potential of various coral species is substantial, the application of metabolic enzymatic assay analysis in characterizing local metabolic adaptation across both depth and habitat is novel. For the purposes of this study, depth is comparable to water turbidity wherein an increase in depth is assumed to mimic an increase in water turbidity<sup>83,84</sup>. These results will augment those of the location analyses wherein the strongest evidence for intraspecific metabolic photoacclimation signatures are anticipated to arise. This inclination stems from the contrast in quality of shallow-water habitat between Punta Caracol and Eric Reef. By comparing the various activities of major metabolic enzymes between depth- and spatial-specific populations of *A. cervicornis* and *P. astreoides*, baselines which characterize the aerobic and fermentative capacities may be established.

## MATERIALS & METHODS

### Sample Collection

*A. cervicornis* branch tips (~10 cm) were harvested from healthy colonies using stainless steel bone cutters. Variations in depth zonation at the Punta Caracol site prevented collection of field population samples at depths exceeding 5 meters. Consequentially, *A. cervicornis* fragments (~10 cm) were collected from Punta Caracol populations at 3 meters and 5 meters rather than at the planned 3 meters and 8 meters. However, *A. cervicornis* populations at Eric Reef and *P. astreoides* did not exhibit this depth-limitation. Healthy colonies were identified at 3 meters and 8 meters, and samples (~4-6 cm) from these populations were harvested using a hammer and chisel. Immediately following fragmentation, divers shuttled the samples in labeled plastic zip-top bags to an accompanying vessel where they were rapidly frozen in dry ice for later analysis. From each depth population, 7 samples were obtained for each coral species ( $n = 7$ ).

### Determination of enzymatic activity of metabolic enzymes

Enzymatic assays are very sensitive to the way samples are processed and to the method used to normalize enzymatic activity as a function of mass. These issues become especially important when working with samples with intrinsically low enzymatic activities such as coral tissues. Thus, considerable effort was placed to optimize protocols to minimize experimental variability as much as possible.

### Tissue Homogenization

The order in which samples were homogenized was determined using a random-number generator. Tissues were separated from their skeletons with homogenization buffer (100 mM Tris buffer pH 7.5 at 20°C) propelled using an airbrush (Paasche Airbrush Company, MIL#3 Millennium Airbrush). Homogenates were sonicated using a cell disrupter (Branson Sonic Power

Company, Sonifier W185D) on dry ice at low-power (45 W) over multiple rest-and-pause cycles to limit any potential warming. The cycles consisted of 30 seconds of sonication followed by 10 seconds of rest on dry ice for a total of 2 minutes and 30 seconds. The resulting crude homogenates were then centrifuged (Eppendorf AG, 5810 R Centrifuge) at 4°C for 15 minutes at 500 relative centrifugal force (RCF) to separate the coral fraction from the zooxanthellae. Following centrifugation, the coral supernatant was transferred to multiple 1.5 mL Eppendorf tubes and flash-frozen under dry ice for storage at -80°C. The zooxanthellae pellets were discarded. Prior to analysis, frozen homogenates were allowed to thaw completely on ice.

### **Enzyme activity assays**

Enzymatic assays for MDH (E.C. 1.1.1.37), LDH (E.C. 1.1.1.27), SDH (E.C. 1.5.1.22), ADH (E.C. 1.5.1.17), and CS (E.C. 2.3.3.1) were performed in triplicate using a SpectraMax iD3 microplate reader (Molecular Devices, LLC) at 27.0 °C in 96-well plates (Corning, Costar\* 96-Well EIA/RIA plates). All enzymatic assays were optimized for corals from Linsmayer and Tresguerres (*unpublished*)<sup>85</sup>. MDH (80 mM imidazole buffer pH 7.0 at 20°C, 100 mM KCl, 0.15 mM NADH, 0.3 mM oxaloacetate), LDH (50 mM imidazole buffer pH 7.0 at 20°C, , 100 mM KCl, 0.15 mM NADH, 1.0 mM sodium pyruvate), SDH (100 mM Tris-HCl buffer pH 7.0 at 20°C, 100 mM glycine, 0.3 mM NADH, 0.3 mM sodium pyruvate), ADH (100 mM imidazole buffer pH 7.0 at 20°C, 200 mM L-alanine, 0.2 mM NADH, 3.0 mM sodium pyruvate), and CS (80 mM Tris buffer pH 8.0 at 20°C, 2.0 Mm MgCl<sub>2</sub>, 0.1 mM DTNB, 0.1 mM acetyl-CoA, 0.5 mM oxaloacetate) reagent concentrations were calculated using a final well reaction volume of 160 µL. Solutions were made fresh daily while sample aliquots thawed completely on ice. Prior to being loaded onto the microplates, all solutions, buffers, homogenates, and dyes were mixed using a vortex mixer (VWR International, Standard Heavy-Duty Vortex Mixer). Blanks

consisted of 150  $\mu\text{L}$  of appropriate enzyme assay medium and 10  $\mu\text{L}$  of homogenization buffer (100 mM Tris buffer pH 7.5 at 20°C) were run in triplicate alongside their corresponding assay. The addition of 10  $\mu\text{L}$  of coral homogenate initiated the enzymatic reactions. MDH, LDH, SDH, and ADH assays were monitored at 340 nm, corresponding to the oxidation of NADH to NAD<sup>+</sup>. CS assays, in contrast, were measured at 412 nm to reflect the formation of TNB from DTNB. SDH and ADH reactions were allowed to run for 30 minutes, while all remaining assays ran for only 10 minutes.

To obtain more accurate measurements, the Bradford protein assay (Bio-Rad Laboratories, Inc., Bradford Assay) methodology was adapted and integrated with the enzymatic assay protocol using a single 96-well plate—a novel development in the field. Containment on a single plate may potentially improve control over spatial and temporal variables affecting absorbance readings when compared to analysis using multiple plates. Further improvements made on the protein assay involved measuring the protein concentration of each experimental well immediately following enzymatic analysis. Doing so yields protein measurements that reflect actual concentrations observed in each well, thereby increasing the accuracy of the final maximum enzymatic activity calculations. On each plate, designated wells containing 150  $\mu\text{L}$  of the appropriate enzyme solution medium were set aside for the construction of a standard curve. In these wells, 10  $\mu\text{L}$  of bovine serum albumin (BSA) of known dilutions (0, 0.138, 0.265, 0.525, 0.720, and 0.891 mg/mL) replaced the 10  $\mu\text{L}$  of coral homogenate used in the experimental wells. The standards were also allowed to run in triplicate. The addition of 40  $\mu\text{L}$  of room-temperature (27.0°C) Bradford dye concentrate to all wells properly diluted the dye to a final reaction volume of 200  $\mu\text{L}$ . Following room-temperature incubation on a shaker (VWR International, 120 V Microplate Shaker) for 5 minutes at 500 RCF, the 96-well plate was loaded

into a microplate absorbance reader (Bio-Rad Laboratories, Inc., iMark Microplate Absorbance Reader). Using the microplate desktop application (Bio-Rad Laboratories, Inc., Microplate Manager 6 Software), absorbance measurements were made as a ratio of 595 nm to 450 nm to better resolve issues of nonlinearity in the Bradford protein assay<sup>86</sup>. Final experimental protein concentrations were accepted when the generated standard curve  $r^2$  value exceeded 0.95.

From these measurements, maximum enzyme activity values were calculated for all samples using Excel (Microsoft, Excel 2016). Enzymatic absorbance measurements spanning the first 60 seconds were excluded to account for the initial fluctuations observed in the datasets. Using a two-sided estimation, the three largest changes in absolute slope were averaged for each replicate. This provided three separate absorbance measurements for each sample, at which point these values were again averaged to yield the final maximum change in absorbance in each individual sample. Blanks were subtracted from these sample averages when in excess of 5% of the observed value. Once standardized to protein concentration, enzyme activities were expressed as nanomole (nmol) substrate converted per milligram protein per minute ( $\text{nmol}^{-1} \text{mg protein}^{-1} \text{min}^{-1}$ ).

### **Statistical analysis**

All analyses performed and all graphs generated for this study were done using the Prism 8 program (Graphpad Software). From the various packages available through Prism 8, the two-way analysis-of-variance (ANOVA) using Tukey post-hoc test was chosen as the appropriate statistical test to determine potential differences in mean enzyme activity maximums between reef location, relative population depths, and their interaction effects across all assays. The decision to employ a parametric test rather than a nonparametric equivalent or permutation is multifaceted. First and foremost, parametric tests are more commonly used and, as a result, are

also well-understood in the vast majority of scientific disciplines<sup>87-90</sup>. Additionally, parametric tests are more robust than their nonparametric counterparts given that the data meets the criteria of equal variance, normality, and sufficiently large and equal samples sizes<sup>88,91-93</sup>. Although sample sizes here are relatively small ( $n < 30$ ), an analysis of the available literature reveals the prevalence of similar statistical assumptions made under experimental designs that closely resemble that of this study. This reflects the notion that the distributions of the actual biological populations are expected to be normal. To supplement, visual methods and evaluation of skewness and kurtosis were used in conjunction with the more formal Shapiro-Wilk test as a means to assess whether the assumptions of normality required for such parametric statistical procedures were met<sup>91,94-98</sup>. Results are shown as mean standard error of the mean ( $\pm$ SEM). Graphical representations of these results are reported in Figure 2 and Figure 3. These graphs are also presented alongside their corresponding two-way ANOVA tables in the Appendix. Tabular results using Tukey's multiple comparisons tests are also provided in the Appendix where significant effects were detected.



## RESULTS

### *A. cervicornis*

The enzymatic activities of *A. cervicornis* from Punta Caracol and Eric Reef from the different depths are shown in Figure 3. No significant differences ( $\alpha = 0.05$ ) in the main effects of relative population depth and reef location, nor in the interaction effect, were detected in LDH, SDH, and CS enzymatic activities for *A. cervicornis*. While LDH, SDH, and CS activities were comparable across both depth and reef location, SDH activity was highly variable with a tendency for higher activities in Punta Caracol samples. On the other hand, there was a significant main effect of reef location on MDH ( $p < 0.001$ ) and ADH ( $p < 0.001$ ) enzymatic activities, both of which were higher in Punta Caracol samples compared to those in Eric Reef (MDH<sub>Punta Caracol</sub> ~30-40 % higher than MDH<sub>Eric Reef</sub>; ADH<sub>Punta Caracol</sub> ~1.5 to 2.0-fold higher than ADH<sub>Punta Caracol</sub>).

### *P. astreoides*

The enzymatic activities of *P. astreoides* from Punta Caracol and Eric Reef from 3 meters and 8 meters are shown in Figure 4. Overall, *P. astreoides* enzymatic activities were 5 to 10-fold higher compared to *A. cervicornis*. As in *A. cervicornis*, there were no significant differences in *P. astreoides* LDH activity ( $\alpha = 0.05$ ) across both main and interaction effects. There was, however, a significant main effect of reef location on the activities of MDH ( $p = 0.006$ ), SDH ( $p < 0.001$ ), and ADH ( $p < 0.001$ ) for this species. In terms of biologically significant results, MDH activity in Eric Reef *P. astreoides* samples was ~1.2 to 1.5-fold higher compared to their Punta Caracol counterparts. In contrast, SDH and ADH activities were >10-fold higher in Punta Caracol compared to Eric Reef. Unique among my dataset was that CS activity demonstrated significant interaction effect between depth and reef location ( $p < 0.001$ ).

To better resolve this interaction effect, a *post hoc* Tukey's multiple comparisons test was employed, which revealed ~5-fold significantly higher CS activity in shallow habitats at Eric Reef ( $p < 0.001$ ) compared to all other locations.

### **Fermentative to aerobic ratios**

Finally, the ratios of fermentative enzymes activities to CS activity were calculated as proxies for relative reliance on fermentative to aerobic capacity (Table 1). Maximum fermentative capacity was represented as the sum of LDH, SDH, and ADH activities, while maximum aerobic capacity was represented as CS activity<sup>99,100</sup>. Smaller ratio values indicate higher aerobic activity relative to fermentative activity and vice versa. *A. cervicornis* ratios are 6 to 7-fold larger in Punta Caracol populations compared to Eric Reef conspecifics. *P. astreoides* ratios follow a similar pattern, although Punta Caracol population ratios are 7 to 40-fold higher in magnitude.

*A. cervicornis*

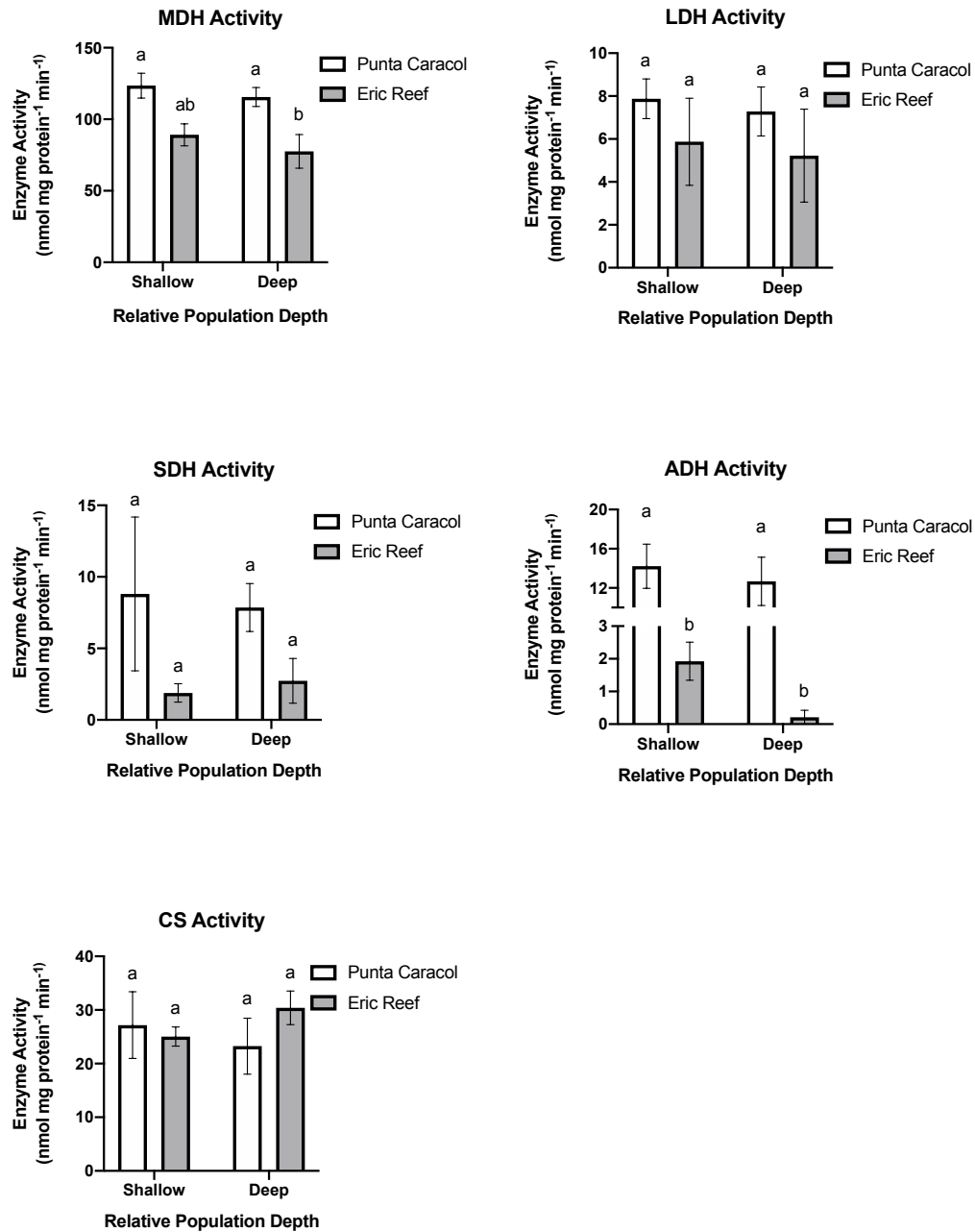


**Figure 3:** Metabolic enzyme activities for *A. cervicornis* from Punta Caracol and Eric Reef. (A) Malate dehydrogenase (MDH), (B) lactate dehydrogenase (LDH), (C) strombine dehydrogenase (SDH), (D) alanopine dehydrogenase (ADH), and (E) citrate synthase (CS). Shallow and deep relative population depths reflect sampling at 3 meters and 8 meters at the Eric Reef site, respectively. At Punta Caracol, shallow and deep relative population depths reflect sampling at 3 meters and 5 meters, respectively. The letters indicate statistical significance (2-way ANOVA;  $n = 7$ ). Values are shown as mean  $\pm$  SEM.

*P. astreoides*

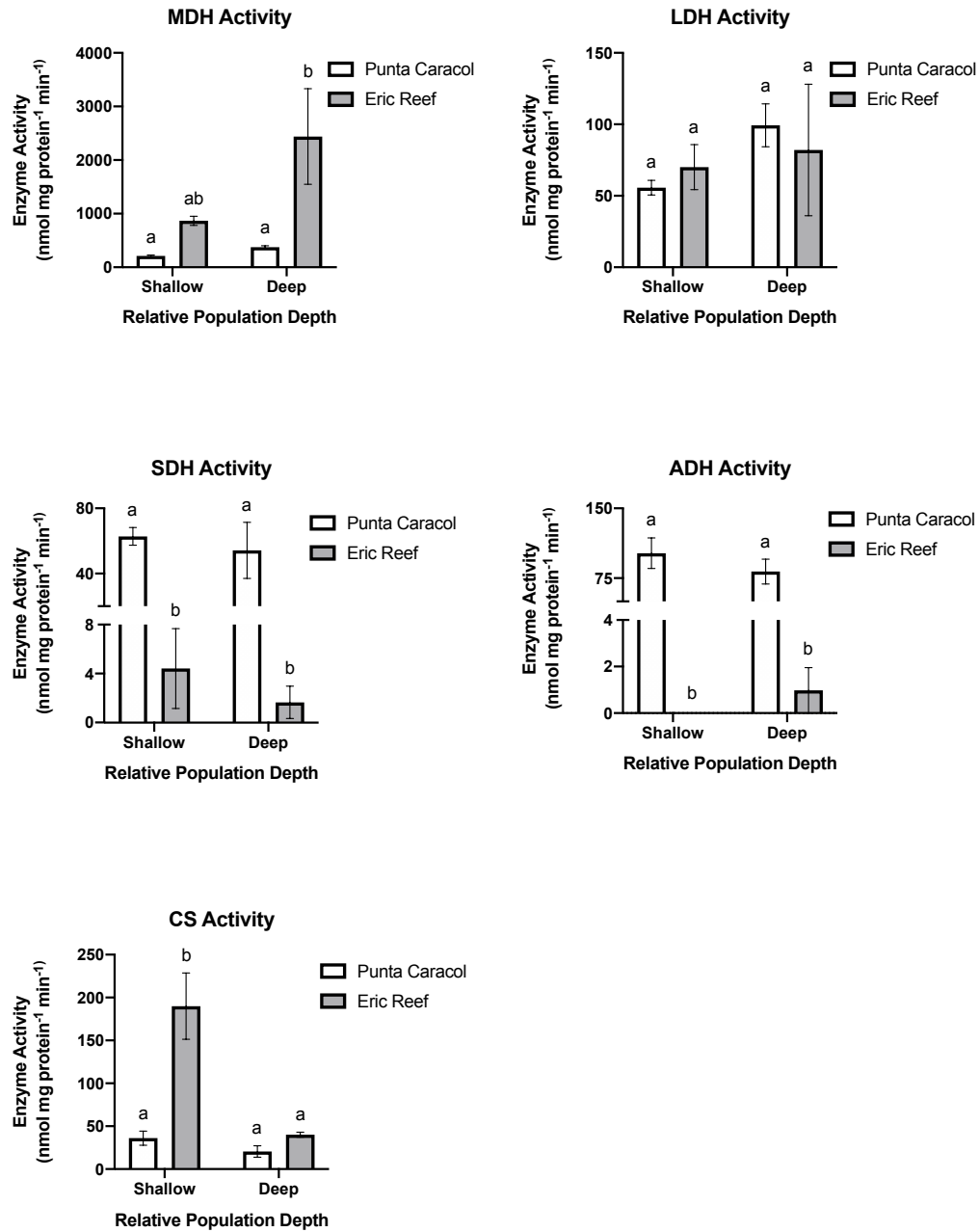


**Figure 4:** Enzymatic activity of malate dehydrogenase (MDH), lactate dehydrogenase (LDH), strombine dehydrogenase (SDH), alanopine dehydrogenase (ADH), and citrate synthase (CS) for *P. astreoides*. Shallow and deep relative population depths reflect sampling at 3 meters and 8 meters, respectively. The letters indicate statistical significance (2-way ANOVA;  $n = 7$ ). Values are shown as mean  $\pm$  SEM.

**Table 1:** Ratios of fermentative to aerobic metabolic capacity for *A. cervicornis* and *P. astreoides*. Smaller LDH+SDH+ADH:CS ratio values are representative of higher aerobic enzyme activity relative to that of fermentative activity and vice versa. Values are shown as mean  $\pm$  SEM.

Coral Species	Reef Location	Depth	LDH + SDH + ADH Activity (nmol mg protein <sup>-1</sup> min <sup>-1</sup> )	CS Activity (nmol mg protein <sup>-1</sup> min <sup>-1</sup> )	Enzyme Activity Ratio
<i>Acropora cervicornis</i>	Punta Caracol	Shallow (3 meters)	30.9 $\pm$ 7.3	27.2 $\pm$ 6.2	1.9 $\pm$ 0.9
		Deep (5 meters)	27.8 $\pm$ 4.6	23.2 $\pm$ 5.2	2.0 $\pm$ 0.8
	Eric Reef	Shallow (3 meters)	9.7 $\pm$ 2.6	25.0 $\pm$ 1.8	0.4 $\pm$ 0.1
		Deep (8 meters)	8.2 $\pm$ 2.2	30.4 $\pm$ 3.1	0.3 $\pm$ 0.1
<i>Porites astreoides</i>	Punta Caracol	Shallow (3 meters)	220.1 $\pm$ 22.8	36.1 $\pm$ 8.2	17.9 $\pm$ 11.9
		Deep (8 meters)	235.4 $\pm$ 37.4	20.5 $\pm$ 6.6	25.6 $\pm$ 9.0
	Eric reef	Shallow (3 meters)	74.4 $\pm$ 18.6	190.0 $\pm$ 38.6	0.6 $\pm$ 0.2
		Deep (8 meters)	84.5 $\pm$ 45.4	40.1 $\pm$ 2.9	2.5 $\pm$ 1.4

## DISCUSSION

The results presented here indicate that the energy metabolic pathways of *A. cervicornis* and *P. astreoides* are tuned to local environmental conditions that, generally, favor fermentation in Punta Caracol—suggested by the higher activities of the various OpDHs. As discussed previously, Punta Caracol is a more turbid lagoon environment subject to elevated and highly variable terrestrial inputs. In contrast, Eric Reef is exposed to the Caribbean, has limited terrestrial influence, and lower turbidity. Consequentially, light dissipates more rapidly with depth at Punta Caracol while the low-turbidity waters at Eric Reef allow for greater light penetration through the water column. Since changes in marine irradiance fields from episodic sediment resuspension on costal coral reefs may reduce the quality and availability of light for weeks<sup>101</sup>, expectations prior to data analysis maintained that Punta Caracol coral populations would exhibit lower overall metabolic activity than those of Eric Reef. Interestingly, this assumption proved invalid in *A. cervicornis*—MDH results indicate ~30 to 40% higher metabolic maximum capacities in Punta Caracol specimens compared to conspecifics from Eric Reef.

Energetically, it is difficult to identify any potential benefits that may explain why *A. cervicornis* communities at Eric Reef, which presumably have access to a larger flux of high-quality PAR, would exhibit lower metabolic maximum capacities compared to conspecifics at Punta Caracol. It may be argued that the *A. cervicornis* populations sampled at Eric Reef are exhibiting metabolic suppression—a physiological adaptation employed by representatives in virtually all animal phyla to reduce energy costs associated with stressful conditions<sup>102</sup>. However, the bioenergetic consequences of this response limits its implementation to short periods<sup>103–105</sup>. Furthermore, a recent study about the impacts of ocean acidification on *Acropora*

*millepora* has suggested that long-term metabolic suppression is associated with elevated fitness costs that makes it infeasible as a lifelong adaptive strategy<sup>106</sup>. A more fitting interpretation may include the effects of ultraviolet light radiation (UVR). Historically, numerous studies have identified UVR exposure as a determinant in the composition and structure of coral reef communities with UVR penetration exceeding depths of 20 meters<sup>107–111</sup>. Exposure of reef organisms to UVR has severe physiological consequences that range from mortality to decreased growth and calcification rates, reduced photosynthesis, changes in respiration, DNA and cytoskeletal damage, oxidative stress, and photoinhibition<sup>112,113</sup>. To combat this, corals have evolved several defensive strategies that may be categorized as either those that prevent UVR from damaging critical cellular constituents or those that counter the negative effects of UVR once they have manifested<sup>114</sup>. Of these preventative strategies, UVR-absorbing compounds are by far the most investigated of the UVR protective mechanisms in corals. These include the family of mycosporine-like amino acids which have been documented in a variety of marine organisms<sup>115</sup> and act as a natural sunscreen and may also function as an antioxidant<sup>116</sup>. Antioxidants belong to the second classification of coral defense against UVR damage by neutralizing reactive oxygen species produced through indirect photodynamic action<sup>117</sup>. While some studies have shown that the manufacturing and maintenance of these various protective compounds represent a significant energetic cost to the organism upon initial exposure to UVR<sup>118</sup>, this may not necessarily be the case for locally-adapted coral populations. One analysis of *Montipora verrucosa* suggests that UVR-acclimated corals do not exhibit high long-term costs associated with respiration<sup>119</sup>. It has been proposed that such conflicting patterns in the literature may reflect differences in microhabitat conditions<sup>120</sup>—likely in combination with variable species-specific responses to the abiotic factors that characterize their microenvironments.

Given that dissolved organic carbon (DOC), suspended sediments, and elevated nutrient loads are well-known absorbers of UVR in seawater<sup>121</sup>, it is unsurprising that these various contributors to water turbidity account for an estimated 70% of UVR attenuation in tropical shallow waters ( $\leq 5$  meters)<sup>122</sup>. To that end, the feculent environment at Punta Caracol may provide resident coral populations sufficient protection from acute physiological stress associated with chronic UVR exposure. However, the consistently higher fermentative capacities of *A. cervicornis* at Punta Caracol relative to conspecifics at Eric Reef do not agree with this assertion. Under such circumstances, metabolic enzyme activities would likely be higher in Eric Reef populations where water column clarity would necessitate the production and maintenance of appropriate UVR-protective compounds at potentially high energetic costs<sup>123</sup>. Conflicting results both here and in the available literature warrant further scientific inquiry regarding the effects of UVR on the biological processes of corals.

Higher overall MDH, LDH, SDH, and ADH activities observed in the *A. cervicornis* populations at Punta Caracol may point to a greater demand for fermentative energy production due to an abundance in available prey and rapid PAR attenuation with depth. Under such conditions, photosynthetic rates are reduced, oxygen is limited, and algae-derived carbon translocation is repressed. To meet survivorship costs, *A. cervicornis* populations at Punta Caracol may be relying more heavily on heterotrophy as a result of increased prey abundance and lower PAR availability. Evidence of heterotrophic feeding as a means to maintain a positive energy balance under light limitation is substantial<sup>30,80,124–129</sup> and fits well within the context of the local adaptation hypothesis. For example, rapid responses in *Turbinaria mesenterina* to perturbations in irradiance suggests that the underlying kinetics of photoacclimation is a significant adaptive factor in the photo-physiology of turbid inshore reefs<sup>130</sup>. Extending this logic



to conspecifics at Eric Reef may also help elucidate the lower maximum enzyme activities detected at this site. Although PAR may be more readily available at Eric Reef, this does not necessarily translate to greater metabolic capacity. It has been observed that zooxanthellae, despite persistent and ideal light conditions, are unable to supply the coral host with a quality food source in nutrient-replete conditions<sup>131</sup>. To that end, *A. cervicornis* populations at Eric Reef may be battling both the energetic costs associated with exposure to UVR and limited availability of high-quality food resources—both of which are plausible conditions in habitats defined by high water column clarity. While empirical evidence supporting direct connections between photosynthesis and heterotrophic feeding is lacking, increased reliance on heterotrophic carbon and nutrient acquisition by the coral host provides one of the more sensible explanations behind the metabolic signatures observed in this thesis.

Unlike *A. cervicornis*, the results of *P. astreoides* enzymatic assays conform well within the boundaries of the depth- and spatial-specific hypothesis. MDH activities are ~1.5-fold higher at Eric Reef than their conspecifics at Punta Caracol—with a dramatically higher mean in the deep-water populations at Eric Reef. Despite its utility as a representative substitute for idealized general metabolic scope, the extent to which the deep-water Eric Reef communities utilize MDH relative to conspecifics and *A. cervicornis* may be elucidated by its role in multiple metabolic pathways including the TCA cycle, gluconeogenesis, malate-aspartate shuttle, and glyoxylate cycle. Nonetheless, trends in *P. astreoides* MDH and CS activities coincide with metabolic interconnections that are worth noting. Published data pertaining to MDH kinetic mechanisms show that citrate acts as both an activator and inhibitor of MDH in conjunction with L-malate and oxaloacetate<sup>132,133</sup>. While the relationship between MDH and citrate may be a contributing factor in the results presented, studies are limited and exclude coral organisms. Furthermore, the

interplay of these various effectors is highly complex<sup>57</sup> and requires further scientific inquiry before any conclusions may be drawn with a reasonable degree of certainty.

Although LDH activity has been previously detected in anemones<sup>134</sup> and cold-water corals<sup>58</sup>, it was absent in a recent study on the tropical reef-building coral *Montipora capitata*<sup>22</sup>. In contrast, the current study consistently detected LDH activity in *A. cervicornis* and *P. astreoides* from all locations and depths and deserves further investigation. Interestingly, LDH activities did not exhibit any significant differences across both factors of reef location and depth in either coral species, suggesting a basal role that is not responsive to environmental variability. The sum all three fermentative terminal dehydrogenases (LDH, SDH, and ADH) among both *P. astreoides* and *A. cervicornis* from Punta Caracol suggest this environment favors fermentation and may potentially be related to heterotrophic food source and PAR availability. CS results from *P. astreoides* also agree with this assertion—most notably in sampled populations inhabiting the shallow-waters of Eric Reef where CS activity is 136.2% greater than their Punta Caracol conspecifics.

Seemingly contradictory results from *A. cervicornis* and *P. astreoides* sampled at Eric Reef most likely reflect a combination of species-specific adaptive response, light availability, and prey preference and abundance. Nevertheless, detectable activities in all enzymatic assays across both coral species regardless of reef location illustrates the adaptability of the coral holobiont to the variability of its local environment. By no means is this concept novel. Experiments on the high-light-adapted corals *Favia fava*, *Plerogyra sinuosa*, and *Goniopora lobate* suggest that these organisms possess and utilize a variety of acclimation mechanisms including fluorescence yields, photosynthetic pigment content, and production of reactive oxygen species protective enzymes as a means of adaptation to the light regimes of their

environment<sup>135</sup>. A comparison of deep water (40 meters) and shallow water (3 meters) *Stylophora pistillata* corals revealed that these colonies are chromatically adapted to the downwelling light of their environments<sup>136</sup> by producing pigments that modify the surface light environment through emission, light scattering, and reflectance<sup>137</sup>. Similarly, an investigation into the differential effects of ultraviolet radiation on green and brown morphologies of *P. astreoides* as a function of depth illustrated the ability of this species to photoacclimate via differential tissue pigment expression<sup>118</sup>. Curiously, these compounds may play a dual role in the photobiological regulation of the coral tissue light environment not only in a photoprotective capacity, but also as photo-enhancers. It has been suggested that coral tissue green fluorescent pigment may convert otherwise harmful UVR into light available for the photosynthesis of zooxanthellae in the endoderm<sup>138</sup>. One study of Red Sea *Leptoseris fragilis* populations postulates that pigments manufactured by the coral host provides its symbiotic algae with additional light by transforming short wavelength light into wavelengths appropriate for photosynthesis—thus elevating the transfer of photosynthetically-fixed carbon from the zooxanthellae to the coral host<sup>139</sup>. The dualities associated with such adaptations denote the magnitude by which abiotic factors shape coral reef communities while simultaneously highlighting the extent in which corals are able to adapt to the highly variable conditions that define their microenvironments.

To better resolve the relative capacities of aerobic and fermentative metabolic pathways, LDH+SDH+ADH:CS ratios were calculated and are presented in Table 1. Smaller LDH+SDH+ADH:CS ratio values are representative of higher aerobic enzyme activity relative to that of fermentative activity and vice versa<sup>140</sup>. These calculations reinforce the dominance of fermentation at Punta Caracol and, to a lesser extent, aerobic metabolism at Eric Reef—

especially for *P. astreoides*. What is more impressive, however, is that the fermentative capacity of *P. astreoides* at Punta Caracol is several-fold larger than that of any other observational group. Interestingly, *A. cervicornis* populations, which historically dominated Caribbean reefs, have been in dramatic decline over the last several decades<sup>141</sup>. While bleaching events and white band disease are widely accepted as the principal culprits<sup>142</sup>, it is worthwhile to consider the loss of *A. cervicornis* in a metabolic framework as well. In the scope and context of this study, the relatively low metabolic capacity of locally-adapted *A. cervicornis* populations illustrate the susceptibility of the species to anomalies in environmental conditions. Without a sufficiently robust and adaptable energy production physiology capable of meeting elevated metabolic demands, it may be possible that *A. cervicornis* numbers will continue to fall with mounting anthropogenic earth and climate alterations. These changes include elevated sediment stress, as *A. cervicornis* is known to lower its net productivity with respect to other coral species studied<sup>143</sup>. This is in stark contrast with *P. astreoides*, which has experienced 50% increased percent reef coverage in Caribbean reefs over a similar timescale<sup>144</sup>. This shift in reef community composition to a more *P. astreoides*-dominated state also coincides with the larger metabolic capacity of this species as determined here—matching known trends of resilience to general stress.

### **Conclusions and future directions**

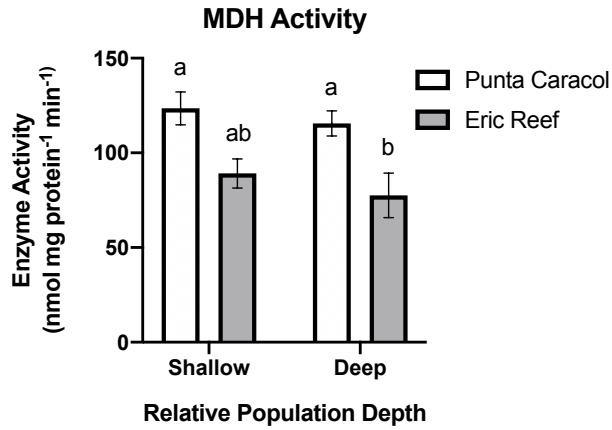
As the degradation of the various earth systems presses onwards, so too does the vanguard of marine biodiversity that is the coral reef. Acting on both local and global scales, the interactions of multiple anthropogenic stressors threaten the very existence of coral reefs as we know them. As in Bocas del Toro, Panama, reef ecosystems around the globe face similar threats of sedimentation and eutrophication. The potential impact these pollutants have on limiting the

critical light resource shallow-water corals depend on demonstrates the need to develop methodologies and baselines to assess coral metabolic potential quickly, precisely, and economically. Gaining this knowledge may prove key in identifying susceptible corals before bleaching and death, thereby allowing the distribution of conservation and management efforts in an effective and resourceful manner. The use of such enzyme assays as bioindicators of stress has been described and shows potential in quantification of hypoxic metabolic stress<sup>22</sup>, highlighting the versatility of this approach.

The significance of this methodology for future coral research efforts lies in the highly complex and interconnected relationships that exist between light, oxygen, and nutrition—all of which help determine the survival of the coral holobiont. Since oxygen sustains highly efficient aerobic metabolism, it is as integral to the vitality of the coral reef system as light. And like light, oxygen availability is dynamic—though fluctuations in oxygen concentrations vary on far greater spatiotemporal scales<sup>65</sup>. Alongside nutrient availability, the interplay of light and oxygen defines almost all aspects of the reef environment, allotting a unique opportunity to detangle the mysteries that have plagued coral researchers and conservationists alike. Enzymatic assay analysis is unique in its potential biological applications across multiple abiotic and biotic factors. The application of enzymatic assay methodologies in this thesis has revealed novel metabolic signatures that may improve the characterization of local reef environments while concomitantly advancing our understanding of coral adaptation to their unique microhabitats.

## APPENDIX

*Acropora cervicornis* MDH



Source of Variation	Interaction	Relative Depth	Reef Location
% of total variation	0.09773	2.875	39.59
P value	0.8416	0.2839	0.0004
P value summary	ns	ns	***
Significant?	No	No	Yes

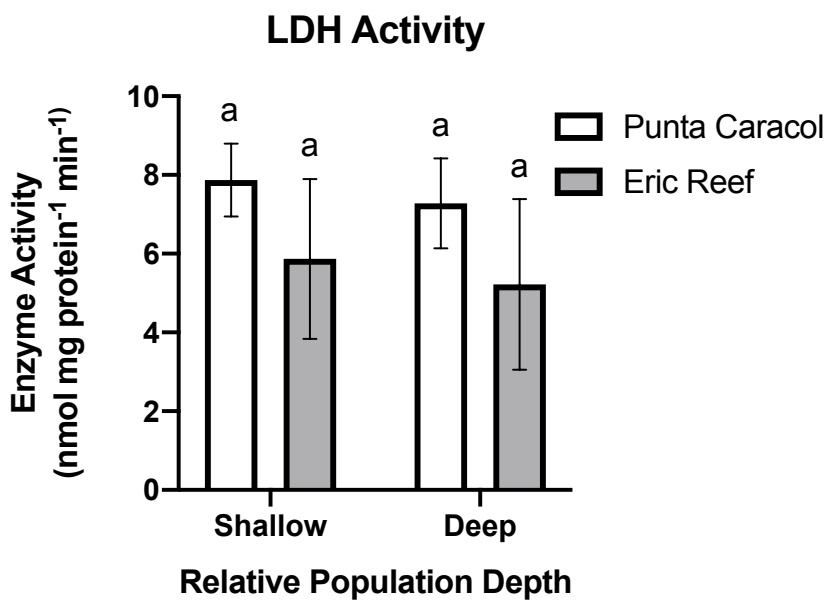
  

ANOVA table	Interaction	Relative Depth	Reef Location	Residual
SS	22.66	666.7	9180	13316
DF	1	1	1	24
MS	22.66	666.7	9180	554.8
F (DFn, DFd)	F (1, 24) = 0.04084	F (1, 24) = 1.202	F (1, 24) = 16.54	
P value	P=0.8416	P=0.2839	P=0.0004	

Tukey's multiple comparisons test	Mean Diff.	95.00% CI of diff.	Significant?	Summary	Adjusted P Value
Shallow:Punta Caracol vs. Shallow:Eric Reef	34.41	-0.3191 to 69.15	No	ns	0.0528
Shallow:Punta Caracol vs. Deep:Punta Caracol	7.960	-26.77 to 42.69	No	ns	0.9206
Shallow:Punta Caracol vs. Deep:Eric Reef	45.97	11.24 to 80.70	Yes	**	0.0065
Shallow:Eric Reef vs. Deep:Punta Caracol	-26.45	-61.19 to 8.279	No	ns	0.1814
Shallow:Eric Reef vs. Deep:Eric Reef	11.56	-23.17 to 46.29	No	ns	0.7955
Deep:Punta Caracol vs. Deep:Eric Reef	38.01	3.279 to 72.74	Yes	*	0.0283

**Figure 5a:** *A. cervicornis* MDH: Graphical representations of the results as reported in Figure 3 presented alongside their corresponding two-way ANOVA tables. Tabular results of Tukey's multiple comparisons tests are also provided where significant effects were detected.

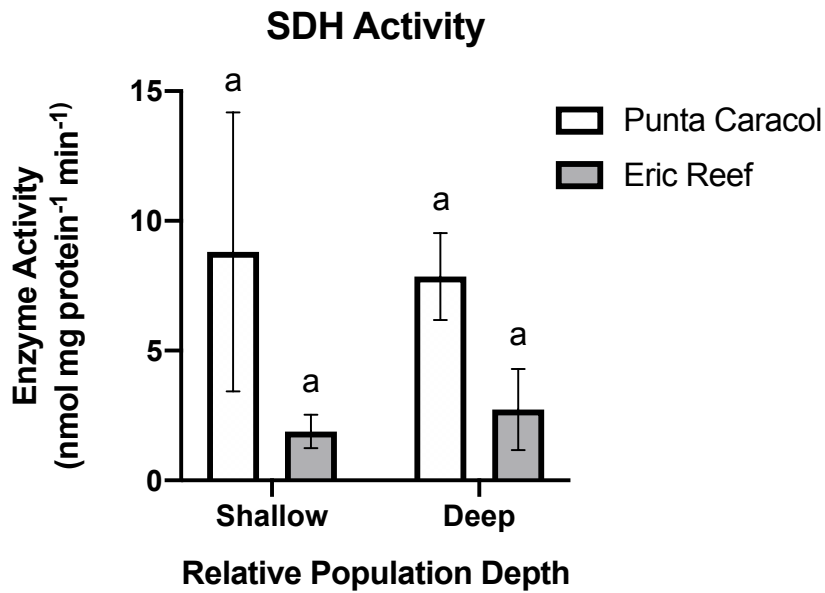


Source of Variation	Interaction	Relative Depth	Reef Location
% of total variation	0.001137	0.5480	5.855
P value	0.9865	0.7111	0.2323
P value summary	ns	ns	ns
Significant?	No	No	No

ANOVA table	Interaction	Relative Depth	Reef Location	Residual
SS	0.005599	2.698	28.83	460.8
DF	1	1	1	24
MS	0.005599	2.698	28.83	19.20
F (DFn, DFd)	F (1, 24) = 0.0002916	F (1, 24) = 0.1405	F (1, 24) = 1.501	
P value	P=0.9865	P=0.7111	P=0.2323	

**Figure 5b:** *A. cervicornis* LDH: Graphical representations of the results as reported in Figure 3 presented alongside their corresponding two-way ANOVA tables.



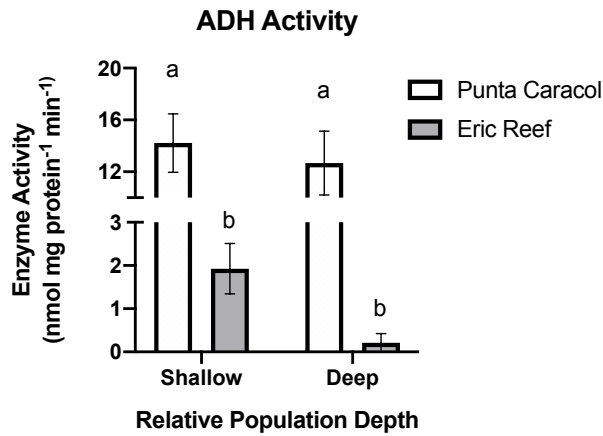
Source of Variation	Interaction	Relative Depth	Reef Location
% of total variation	0.3273	0.001156	14.85
P value	0.7635	0.9857	0.0515
P value summary	ns	ns	ns
Significant?	No	No	No

ANOVA table	Interaction	Relative Depth	Reef Location	Residual
SS	5.596	0.01976	253.9	1450
DF	1	1	1	24
MS	5.596	0.01976	253.9	60.42
F (DFn, DFd)	F (1, 24) = 0.09260	F (1, 24) = 0.0003271	F (1, 24) = 4.202	
P value	P=0.7635	P=0.9857	P=0.0515	

**Figure 5c:** *A. cervicornis* SDH: Graphical representations of the results as reported in Figure 3 presented alongside their corresponding two-way ANOVA tables.





Source of Variation	Interaction	Relative Depth	Reef Location
% of total variation	0.003079	1.185	68.11
P value	0.9613	0.3455	<0.0001
P value summary	ns	ns	****
Significant?	No	No	Yes

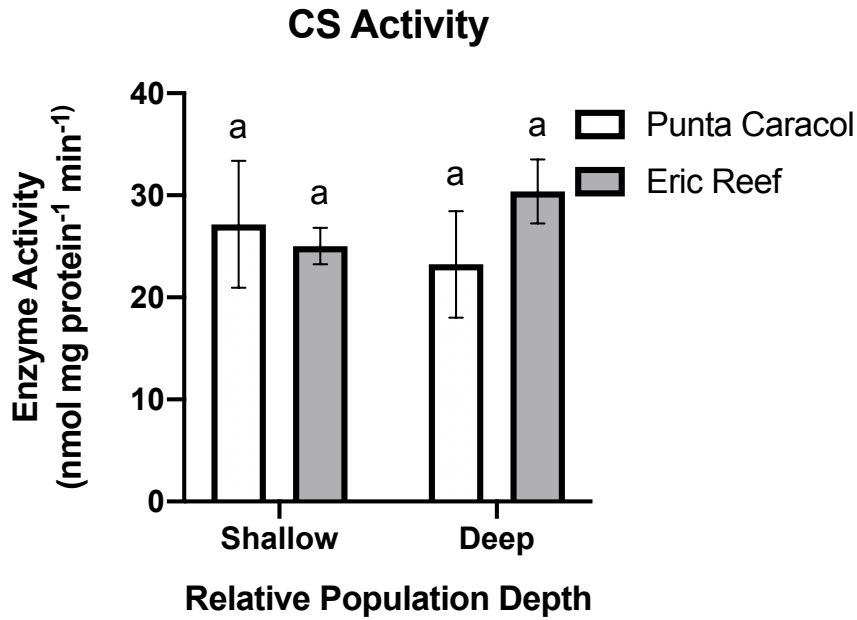
  

ANOVA table	Interaction	Relative Depth	Reef Location	Residual
SS	0.04847	18.65	1072	483.3
DF	1	1	1	24
MS	0.04847	18.65	1072	20.14
F (DFn, DFd)	F (1, 24) = 0.002407	F (1, 24) = 0.9261	F (1, 24) = 53.25	
P value	P=0.9613	P=0.3455	P<0.0001	

Tukey's multiple comparisons test	Mean Diff.	95.00% CI of diff.	Significant?	Summary	Adjusted P Value
Shallow:Punta Caracol vs. Shallow:Eric Reef	12.29	5.676 to 18.91	Yes	***	0.0002
Shallow:Punta Caracol vs. Deep:Punta Caracol	1.549	-5.068 to 8.166	No	ns	0.9160
Shallow:Punta Caracol vs. Deep:Eric Reef	14.01	7.392 to 20.63	Yes	****	<0.0001
Shallow:Eric Reef vs. Deep:Punta Caracol	-10.74	-17.36 to -4.127	Yes	***	0.0008
Shallow:Eric Reef vs. Deep:Eric Reef	1.715	-4.901 to 8.332	No	ns	0.8901
Deep:Punta Caracol vs. Deep:Eric Reef	12.46	5.843 to 19.08	Yes	***	0.0001

**Figure 5d:** *A. cervicornis* ADH: Graphical representations of the results as reported in Figure 3 presented alongside their corresponding two-way ANOVA tables. Tabular results of Tukey's multiple comparisons tests are also provided where significant effects were detected.

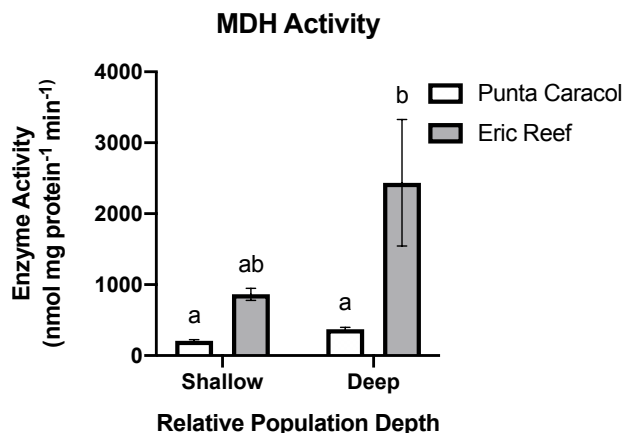


Source of Variation	Interaction	Relative Depth	Reef Location
% of total variation	4.285	0.1010	1.252
P value	0.3069	0.8740	0.5778
P value summary	ns	ns	ns
Significant?	No	No	No

ANOVA table	Interaction	Relative Depth	Reef Location	Residual
SS	150.7	3.551	44.04	3319
DF	1	1	1	24
MS	150.7	3.551	44.04	138.3
F (DFn, DFd)	F (1, 24) = 1.090	F (1, 24) = 0.02568	F (1, 24) = 0.3185	
P value	P=0.3069	P=0.8740	P=0.5778	

**Figure 5e:** *A. cervicornis* CS: Graphical representations of the results as reported in Figure 3 presented alongside their corresponding two-way ANOVA tables.

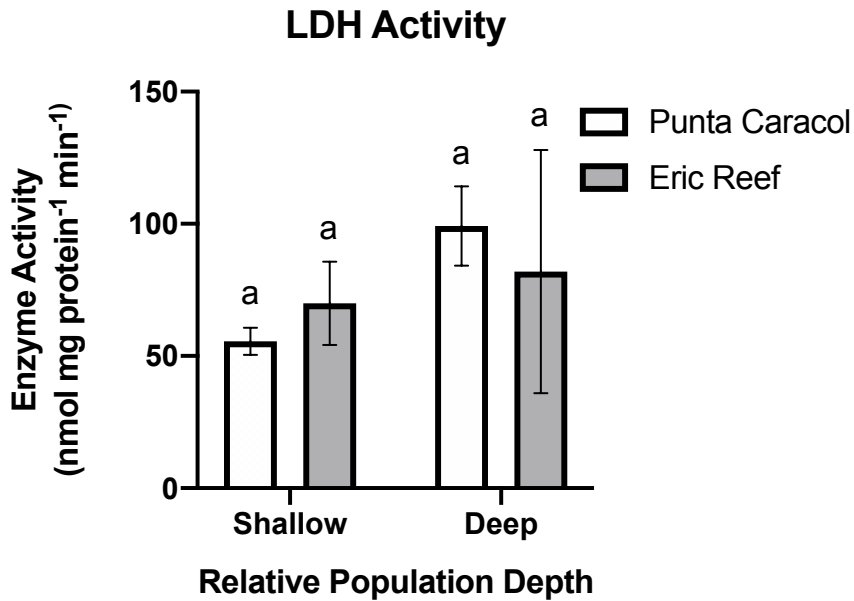


Source of Variation	Interaction	Relative Depth	Reef Location
% of total variation	6.296	9.499	23.38
P value	0.1281	0.0647	0.0057
P value summary	ns	ns	**
Significant?	No	No	Yes

ANOVA table	Interaction	Relative Depth	Reef Location	Residual
SS	3485421	5258733	12942912	33676041
DF	1	1	1	24
MS	3485421	5258733	12942912	1403168
F (DFn, DFd)	F (1, 24) = 2.484	F (1, 24) = 3.748	F (1, 24) = 9.224	
P value	P=0.1281	P=0.0647	P=0.0057	

Tukey's multiple comparisons test	Mean Diff.	95.00% CI of diff.	Significant?	Summary	Adjusted P Value
Shallow:Punta Caracol vs. Shallow:Eric Reef	-654.1	-2401 to 1093	No	ns	0.7320
Shallow:Punta Caracol vs. Deep:Punta Caracol	-161.1	-1908 to 1586	No	ns	0.9941
Shallow:Punta Caracol vs. Deep:Eric Reef	-2227	-3973 to -479.8	Yes	**	0.0089
Shallow:Eric Reef vs. Deep:Punta Caracol	493.0	-1254 to 2240	No	ns	0.8633
Shallow:Eric Reef vs. Deep:Eric Reef	-1572	-3319 to 174.3	No	ns	0.0883
Deep:Punta Caracol vs. Deep:Eric Reef	-2065	-3812 to -318.7	Yes	*	0.0163

**Figure 6a:** *P. astreoides* MDH: Graphical representations of the results as reported in Figure 4 presented alongside their corresponding two-way ANOVA tables. Tabular results of Tukey's multiple comparisons tests are also provided where significant effects were detected.

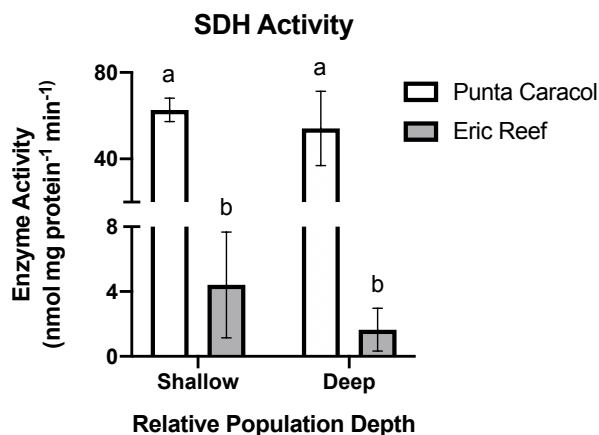


Source of Variation	Interaction	Relative Depth	Reef Location
% of total variation	1.502	4.615	0.01286
P value	0.5413	0.2881	0.9548
P value summary	ns	ns	ns
Significant?	No	No	No

ANOVA table	Interaction	Relative Depth	Reef Location	Residual
SS	1757	5399	15.04	109801
DF	1	1	1	24
MS	1757	5399	15.04	4575
F (DFn, DFd)	F (1, 24) = 0.3840	F (1, 24) = 1.180	F (1, 24) = 0.003287	
P value	P=0.5413	P=0.2881	P=0.9548	

**Figure 6b:** *P. astreoides* LDH: Graphical representations of the results as reported in Figure 4 presented alongside their corresponding two-way ANOVA tables.

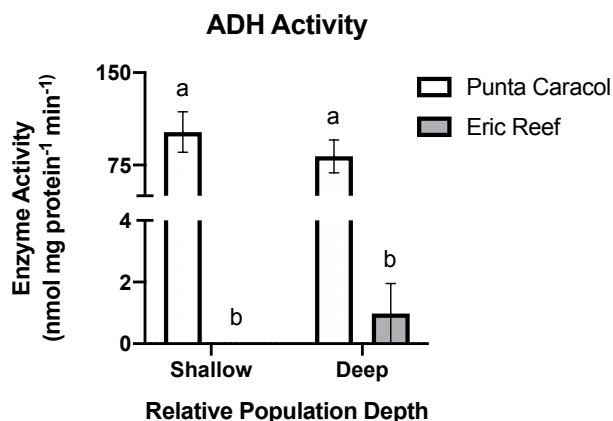


Source of Variation	Interaction	Relative Depth	Reef Location
% of total variation	0.1642	0.6269	59.84
P value	0.7545	0.5423	<0.0001
P value summary	ns	ns	****
Significant?	No	No	Yes

ANOVA table	Interaction	Relative Depth	Reef Location	Residual
SS	58.86	224.8	21455	14116
DF	1	1	1	24
MS	58.86	224.8	21455	588.2
F (DFn, DFd)	F (1, 24) = 0.1001	F (1, 24) = 0.3822	F (1, 24) = 36.48	
P value	P=0.7545	P=0.5423	P<0.0001	

Tukey's multiple comparisons test	Mean Diff.	95.00% CI of diff.	Significant?	Summary	Adjusted P Value
<b>Shallow:Punta Caracol vs. Shallow:Eric Reef</b>	58.26	22.50 to 94.02	Yes	***	0.0008
<b>Shallow:Punta Caracol vs. Deep:Punta Caracol</b>	8.566	-27.19 to 44.33	No	ns	0.9107
<b>Shallow:Punta Caracol vs. Deep:Eric Reef</b>	61.03	25.27 to 96.79	Yes	***	0.0005
<b>Shallow:Eric Reef vs. Deep:Punta Caracol</b>	-49.70	-85.46 to -13.93	Yes	**	0.0042
<b>Shallow:Eric Reef vs. Deep:Eric Reef</b>	2.767	-32.99 to 38.53	No	ns	0.9965
<b>Deep:Punta Caracol vs. Deep:Eric Reef</b>	52.46	16.70 to 88.22	Yes	**	0.0025

**Figure 6c:** *P. astreoides* SDH: Graphical representations of the results as reported in Figure 4 presented alongside their corresponding two-way ANOVA tables. Tabular results of Tukey's multiple comparisons tests are also provided where significant effects were detected.

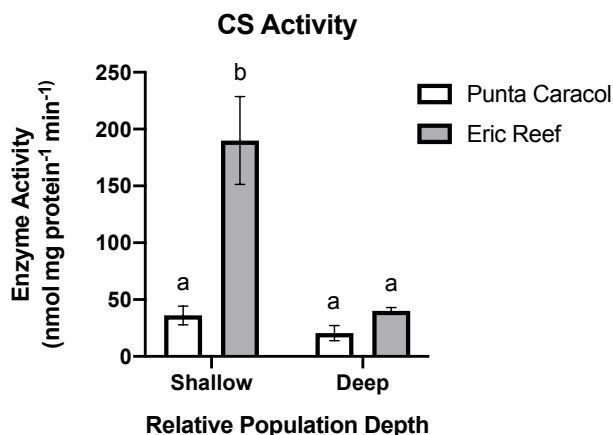


Source of Variation	Interaction	Relative Depth	Reef Location
% of total variation	0.9519	0.7806	74.46
P value	0.3371	0.3838	<0.0001
P value summary	ns	ns	****
Significant?	No	No	Yes

ANOVA table	Interaction	Relative Depth	Reef Location	Residual
SS	748.3	613.7	58533	18716
DF	1	1	1	24
MS	748.3	613.7	58533	779.8
F (DFn, DFd)	F (1, 24) = 0.9596	F (1, 24) = 0.7869	F (1, 24) = 75.06	
P value	P=0.3371	P=0.3838	P<0.0001	

Tukey's multiple comparisons test	Mean Diff.	95.00% CI of diff.	Significant?	Summary	Adjusted P Value
Shallow:Punta Caracol vs. Shallow:Eric Reef	101.8	60.61 to 143.0	Yes	****	<0.0001
Shallow:Punta Caracol vs. Deep:Punta Caracol	19.70	-21.47 to 60.88	No	ns	0.5597
Shallow:Punta Caracol vs. Deep:Eric Reef	100.8	59.63 to 142.0	Yes	****	<0.0001
Shallow:Eric Reef vs. Deep:Punta Caracol	-82.08	-123.3 to -40.90	Yes	****	<0.0001
Shallow:Eric Reef vs. Deep:Eric Reef	-0.9765	-42.15 to 40.20	No	ns	0.9999
Deep:Punta Caracol vs. Deep:Eric Reef	81.10	39.93 to 122.3	Yes	****	<0.0001

**Figure 6d:** *P. astreoides* ADH: Graphical representations of the results as reported in Figure 4 presented alongside their corresponding two-way ANOVA tables. Tabular results of Tukey's multiple comparisons tests are also provided where significant effects were detected.



Source of Variation	Interaction	Relative Depth	Reef Location
% of total variation	15.80	23.98	26.36
P value	0.0027	0.0004	0.0002
P value summary	**	***	***
Significant?	Yes	Yes	Yes

ANOVA table	Interaction	Relative Depth	Reef Location	Residual
SS	31560	47889	52644	67602
DF	1	1	1	24
MS	31560	47889	52644	2817
F (DFn, DFd)	F (1, 24) = 11.20	F (1, 24) = 17.00	F (1, 24) = 18.69	
P value	P=0.0027	P=0.0004	P=0.0002	

Tukey's multiple comparisons test	Mean Diff.	95.00% CI of diff.	Significant?	Summary	Adjusted P Value
Shallow:Punta Caracol vs. Shallow:Eric Reef	-153.9	-232.1 to -75.61	Yes	****	<0.0001
Shallow:Punta Caracol vs. Deep:Punta Caracol	15.57	-62.69 to 93.82	No	ns	0.9460
Shallow:Punta Caracol vs. Deep:Eric Reef	-4.009	-82.27 to 74.25	No	ns	0.9990
Shallow:Eric Reef vs. Deep:Punta Caracol	169.4	91.17 to 247.7	Yes	****	<0.0001
Shallow:Eric Reef vs. Deep:Eric Reef	149.9	71.60 to 228.1	Yes	***	0.0001
Deep:Punta Caracol vs. Deep:Eric Reef	-19.57	-97.83 to 58.68	No	ns	0.8999

**Figure 6e:** *P. astreoides* CS: Graphical representations of the results as reported in Figure 4 presented alongside their corresponding two-way ANOVA tables. Tabular results of Tukey's multiple comparisons tests are also provided where significant effects were detected.

This Thesis is coauthored with Hassibi, Cameron M., Tresguerres, and Kline, David I. The thesis author was the principle researcher/author of the Thesis.

## REFERENCES

1. Smith, J. E., Brainard, R., Carter, A., Grillo, S., Edwards, C., Harris, J., Lewis, L., Obura, D., Rohwer, F., Sala, E., Vroom, P. S. & Sandin, S. Re-evaluating the health of coral reef communities: baselines and evidence for human impacts across the central Pacific. *Proc. R. Soc. B Biol. Sci.* **283**, 20151985 (2016).
2. De'ath, G., Fabricius, K. E., Sweatman, H. & Puotinen, M. The 27-year decline of coral cover on the Great Barrier Reef and its causes. *Proc. Natl. Acad. Sci.* **109**, 17995–17999 (2012).
3. Porter, J. W. & Ouida, M. W. Quantification of loss and change in Floridian reef coral populations. *Am. Zool.* **640**, 625–640 (1992).
4. Lough, J. M. 10th Anniversary Review: A changing climate for coral reefs. *J. Environ. Monit.* **10**, 21–29 (2008).
5. Moberg, F. & Folke, C. Ecological goods and services of coral reef ecosystems. *Ecol. Econ.* **29**, 215–233 (1999).
6. Sala, E. & Knowlton, N. Global Marine Biodiversity Trends. *Annu. Rev. Environ. Resour.* **31**, 93–122 (2006).
7. *Economic Values of Coral Reefs, Mangroves, and Seagrasses.* (2008). doi:10.1111/j.1468-2982.2004.00641.x
8. Lesser, M. P., Marc, S., Michael, S., Michiko, O., Gates, R. D. & Andrea, G. Photoacclimatization by the coral *Montastraea cavernosa* in the mesophotic zone: Light, food, and genetics. *Ecology* **91**, 990–1003 (2010).
9. Smith, S. V. Coral-reef area and the contributions of reefs to processes and resources of the world's oceans. *Nature* **273**, 225–226 (1978).
10. Wear, S. L. Missing the boat: Critical threats to coral reefs are neglected at global scale. *Mar. Policy* **74**, 153–157 (2016).
11. Fisher, R., Radford, B. T., Knowlton, N., Brainard, R. E., Michaelis, F. B. & Caley, M. J. Global mismatch between research effort and conservation needs of tropical coral reefs. *Conserv. Lett.* **4**, 64–72 (2011).
12. Miloslavich, P., Klein, E., Díaz, J. M., Hernández, C. E., Bigatti, G., Campos, L., Artigas, F., Castillo, J., Penchaszadeh, P. E., Neill, P. E., Carranza, A., Retana, M. V., Díaz de Astarloa, J. M., Lewis, M., Yorio, P., Piriz, M. L., Rodríguez, D., Valentin, Y. Y., Gamboa, L. & Martín, A. Marine biodiversity in the Atlantic and Pacific coasts of South America: Knowledge and gaps. *PLoS One* **6**, (2011).



13. Hughes, T. P., Baird, A. H., Bellwood, D. R., Card, M., Connolly, S. R., Folke, C., Grosberg, R., Hoegh-Guldberg, O., Jackson, J. B. C., Kleypas, J., Lough, J. M., Marshall, P., Nyström, M., Palumbi, S. R., Pandolfi, J. M., Rosen, B. & Roughgarden, J. Climate change, human impacts, and the resilience of coral reefs. *Science (80-. )*. **301**, 929–933 (2003).
14. Gaines, S. D., White, C., Carr, M. H. & Palumbi, S. R. Designing marine reserve networks for both conservation and fisheries management. *Proc. Natl. Acad. Sci.* **107**, 18286–18293 (2010).
15. Malcolm, H. A., Foulsham, E., Pressey, R. L., Jordan, A., Davies, P. L., Ingleton, T., Johnstone, N., Hessey, S. & Smith, S. D. A. Selecting zones in a marine park: Early systematic planning improves cost-efficiency; combining habitat and biotic data improves effectiveness. *Ocean Coast. Manag.* **59**, 1–12 (2012).
16. Davy, S. K., Allemand, D. & Weis, V. M. Cell Biology of Cnidarian-Dinoflagellate Symbiosis. *Microbiol. Mol. Biol. Rev.* **76**, 229–261 (2012).
17. Barott, K. L., Barron, M. E. & Tresguerres, M. Identification of a molecular pH sensor in coral. *Proc. R. Soc. B* **284**, 1–8 (2017).
18. Barott, K. L., Perez, S. O., Linsmayer, L. B. & Tresguerres, M. Differential localization of ion transporters suggests distinct cellular mechanisms for calcification and photosynthesis between two coral species. *Am. J. Physiol. - Regul. Integr. Comp. Physiol.* **309**, R235–R246 (2015).
19. Downs, C. A., Woodley, C. M., Richmond, R. H., Lanning, L. L. & Owen, R. Shifting the paradigm of coral-reef ‘health’ assessment. *Mar. Pollut. Bull.* **51**, 486–494 (2005).
20. Weis, V. M. & Allemand, D. What determines coral health? *Science (80-. )*. **324**, 1153–1155 (2009).
21. Weis, V. M., Davy, S. K., Hoegh-Guldberg, O., Rodriguez-Lanetty, M. & Pringle, J. R. Cell biology in model systems as the key to understanding corals. *Trends Ecol. Evol.* **23**, 369–376 (2008).
22. Murphy, J. W. A. & Richmond, R. H. Changes to coral health and metabolic activity under oxygen deprivation. *PeerJ* **4**, 1–16 (2016).
23. Downs, C. A., Mueller, E., Phillips, S., Fauth, J. E. & Woodley, C. M. A molecular biomarker system for assessing the health of coral (*Montastraea faveolata*) during heat stress. *Mar. Biotechnol.* **2**, 533–544 (2000).
24. Kimura, A., Celani, A., Nagao, H., Stasevich, T. & Nakamura, K. Estimating cellular parameters through optimization procedures: Elementary principles and applications. *Front. Physiol.* **6**, 1–9 (2015).

25. Goffredo, S., Mattioli, G. & Zaccanti, F. Growth and population dynamics model of the Mediterranean solitary coral *Balanophyllia europaea* (Scleractinia, Dendrophylliidae). *Coral Reefs* **23**, 433–443 (2004).
26. Hunter, C. L. Genotypic Variation and Clonal Structure in Coral Populations with Different Disturbance Histories. *Evolution (N. Y.)* **47**, 1213–1228 (1993).
27. Romano, S. L. & Palumbi, S. R. Evolution of Scleractinian Corals Inferred from Molecular Systematics. *Science (80-. )* **271**, 640–642 (1996).
28. Stolarski, J., Kitahara, M. V., Miller, D. J., Cairns, S. D., Mazur, M. & Meibom, A. The ancient evolutionary origins of Scleractinia revealed by azooxanthellate corals. *BMC Evol. Biol.* **11**, (2011).
29. Veron, J., Stafford-Smith, M., DeVantier, L. & Turak, E. Overview of distribution patterns of zooxanthellate Scleractinia. *Front. Mar. Sci.* **2**, 1–19 (2015).
30. Wijgerde, T., Jurriaans, S., Hoofd, M., Verreth, J. A. J. & Osinga, R. Oxygen and Heterotrophy Affect Calcification of the Scleractinian Coral *Galaxea fascicularis*. *PLoS One* **7**, 1–6 (2012).
31. White, J. S. S. & O'Donnell, J. L. Indirect effects of a key ecosystem engineer alter survival and growth of foundation coral species. *Ecology* **91**, 3538–3548 (2010).
32. Boogert, N. J., Paterson, D. M. & Laland, K. N. The Implications of Niche Construction and Ecosystem Engineering for Conservation Biology. *Bioscience* **56**, 570 (2006).
33. Roth, M. S. The engine of the reef: Photobiology of the coral-algal symbiosis. *Front. Microbiol.* **5**, 1–22 (2014).
34. Colombo-Pallotta, M. F., Rodríguez-Román, A. & Iglesias-Prieto, R. Calcification in bleached and unbleached *Montastraea faveolata*: Evaluating the role of oxygen and glycerol. *Coral Reefs* **29**, 899–907 (2010).
35. Hochachka, Peter W., Somero, G. N. *Biochemical Adaptation. Mechanism and Process in Physiological Evolution.* (Princeton University Press, 2002).
36. Hochachka, P. W. Fuels and pathways as designed systems for support of muscle work. *J. Exp. Biol.* **115**, 149–164 (1985).
37. Bonora, M., Patergnani, S., Rimessi, A., de Marchi, E., Suski, J. M., Bononi, A., Giorgi, C., Marchi, S., Missiroli, S., Poletti, F., Wieckowski, M. R. & Pinton, P. ATP synthesis and storage. *Purinergic Signal.* **8**, 343–357 (2012).
38. Grieshaber, M. K., Hardewig, I., Kreutzer, U. & Portner, H. O. Physiological and

- metabolic responses to hypoxia in invertebrates. *Rev.Physiol.Biochem.Pharmacol.* **125**, 43–145 (1994).
39. Gäde, G. & Grieshaber, M. K. Pyruvate reductases catalyze the formation of lactate and opines in anaerobic invertebrates. *Comp. Biochem. Physiol.* **83B**, 255–272 (1986).
  40. Livingstone, D. R. Invertebrate and vertebrate pathways of anaerobic metabolism: evolutionary considerations. *J. Geol. Soc. London.* **140**, 27–37 (1983).
  41. Fields, J. H. A. & Storey, K. B. Tissue-specific alanopine dehydrogenase from the gill and strombine dehydrogenase from the foot muscle of the cherrystone clam *Mercenaria mercenaria* (Linn.). *J. Exp. Mar. Bio. Ecol.* **105**, 175–185 (1987).
  42. Fields, J. H. A. & Hochachka, P. W. Purification and properties of alanopine dehydrogenase from the adductor muscle of the oyster, *Crassostrea gigas* (Mollusca, Bivalvia). *Eur. J. Biochem.* **114**, 615–621 (1981).
  43. Kreutzer, U., Siegmund, B. R. & Grieshaber, M. K. Parameters controlling opine formation during muscular activity and environmental hypoxia. *J. Comp. Physiol. B* **159**, 617–628 (1989).
  44. Fields, J. H. A. Alternatives to lactic acid: Possible advantages. *J. Exp. Zool.* **228**, 445–457 (1983).
  45. Weihrauch, D. & Donnell, M. O. *Acid-Base Balance and Nitrogen Excretion in Invertebrates*. (2017). doi:10.1109/ESSCIRC.2014.6942036
  46. Harcet, M., Perina, D. & Pleše, B. Opine dehydrogenases in marine invertebrates. *Biochem. Genet.* **51**, 666–676 (2013).
  47. Fields, J. H. A. & Quinn, J. F. Some theoretical considerations on cytosolic redox balance during anaerobiosis in marine invertebrates. *J. Theor. Biol.* **88**, 35–45 (1981).
  48. Nelson, D. L. & Cox, M. M. *Lehninger Principles of Biochemistry*. (W. H. Freeman and Company, 2008).
  49. Lee, A. C., Lee, K. T. & Pan, L. Y. Purification and kinetic characteristics of strombine dehydrogenase from the foot muscle of the hard clam (*Meretrix lusoria*). *Comp. Biochem. Physiol. Part B* **158**, 38–45 (2011).
  50. Leclère, L. & Röttinger, E. Diversity of Cnidarian Muscles: Function, Anatomy, Development and Regeneration. *Front. Cell Dev. Biol.* **4**, 1–22 (2017).
  51. Hagerman, L. Physiological flexibility; a necessity for life in anoxic and sulphidic habitats. *Recruit. Colon. Phys. Forcing Mar. Biol. Syst.* 241–254 (2013). doi:10.1007/978-94-017-2864-5\_20

52. Sørensen, C., Munday, P. L. & Nilsson, G. E. Aerobic vs. anaerobic scope: Sibling species of fish indicate that temperature dependence of hypoxia tolerance can predict future survival. *Glob. Chang. Biol.* **20**, 724–729 (2014).
53. Somero, G. N., Lockwood, B. L. & Tomanek, L. *Biochemical Adaptation: Response to Environmental Challenges from Life's Origins to the Anthropocene*. (Sinauer Associates, 2017).
54. Childress, J. J. & Somero, G. N. Depth-related enzymic activities in muscle, brain and heart of deep-living pelagic marine teleosts. *Mar. Biol.* **52**, 273–283 (1979).
55. Dahlhoff, E. P., Stillman, J. H. & Menge, B. A. Physiological community ecology: Variation in metabolic activity of ecologically important rocky intertidal invertebrates along environmental gradients. *Integr. Comp. Biol.* **42**, 862–871 (2002).
56. de Zwaan, A., Holwerda, D. A. & Veenhof, P. R. Anaerobic malate metabolism in mitochondria of the sea mussel *Mytilus edulis*. *Mar. Biol. Lett.* **2**, 131–140 (1981).
57. Minárik, P., Tomašková, N., Kollárová, M. & Antalík, M. Malate Dehydrogenases - Structure and function. *Gen. Physiol. Biophys.* **21**, 257–265 (2002).
58. Henry, L. V. & Torres, J. J. Metabolism of an Antarctic solitary coral, *Flabellum impensum*. *J. Exp. Mar. Bio. Ecol.* **449**, 17–21 (2013).
59. Wang, X. M., Soetaert, K., Peirs, P., Kalai, M., Fontaine, V., Dehaye, J. P. & Lefèvre, P. Biochemical Analysis of the NAD<sup>+</sup>-Dependent Malate Dehydrogenase, a Substrate of Several Serine/Threonine Protein Kinases of *Mycobacterium tuberculosis*. *PLoS One* **10**, e0123327 (2015).
60. Dasika, S. K., Vinnakota, K. C. & Beard, D. A. Characterization of the kinetics of cardiac cytosolic malate dehydrogenase and comparative analysis of cytosolic and mitochondrial isoforms. *Biophys. J.* **108**, 420–430 (2015).
61. Liu, L., Zhuge, X., Shin, H. D., Chen, R. R., Li, J., Du, G. & Chen, J. Improved production of propionic acid in *Propionibacterium jensenii* via combinational overexpression of glycerol dehydrogenase and malate dehydrogenase from *Klebsiella pneumoniae*. *Appl. Environ. Microbiol.* **81**, 2256–2264 (2015).
62. Birktoft, J. J., Fu, Z., Carnahan, G. E., Rhodes, G., Roderick, S. L. & Banaszak, L. J. Comparison of the molecular structures of cytoplasmic and mitochondrial malate dehydrogenase. *Biochem. Soc. Trans.* **17**, 301–304 (1989).
63. Dawson, A. G. Oxidation of cytosolic NADH formed during aerobic metabolism in mammalian cells. *Trends Biochem. Sci.* **4**, 171–176 (1979).

64. Muscatine, L. & Porter, J. W. Reef Corals: Mutualistic Symbioses Adapted to Nutrient-Poor Environments. *Bioscience* **27**, 454–460 (1977).
65. Nelson, H. R. & Altieri, A. H. Oxygen: the universal currency on coral reefs. *Coral Reefs* **38**, 177–198 (2019).
66. Dodds, L. A., Roberts, J. M., Taylor, A. C. & Marubini, F. Metabolic tolerance of the cold-water coral *Lophelia pertusa* (Scleractinia) to temperature and dissolved oxygen change. *J. Exp. Mar. Bio. Ecol.* **349**, 205–214 (2007).
67. Kuhl, M., Cohen, Y., Dalsgaard, T., Jorgensen, B. B. & Revsbech, N. P. Microenvironment and photosynthesis of zooxanthellae in scleractinian corals studied with microsensors for O<sub>2</sub>, pH and light. *Mar. Ecol. Prog. Ser.* **117**, 159–177 (1995).
68. Rands, M. L., Douglas, A. E., Loughman, B. C. & Ratcliffe, R. G. Avoidance of Hypoxia in a Cnidarian Symbiosis by Algal Photosynthetic Oxygen. *Biol. Bull.* **182**, 159–162 (1992).
69. Dubinsky, Z. & Stambler, N. Light as a source of information and energy in Zooxanthellae corals. *Coral Reefs An Ecosyst. Transit.* 1–552 (2011). doi:10.1007/978-94-007-0114-4
70. Falkowski, P. G., Dubinsky, Z., Muscatine, L. & Porter, J. W. Light and the Bioenergetics of a Symbiotic Coral. *Bioscience* **34**, 705–709 (1984).
71. Muscatine, L., Falkowski, P. G., Porter, J. W. & Dubinsky, Z. Primary production and photoadaptation in light- and shade-adapted colonies of the symbiotic coral, *Stylophora pistillata*. *Proc. R. Soc. B Biol. Sci.* **222**, 161–180 (1984).
72. Muscatine, L., Falkowski, P. G., Porter, J. W. & Dubinsky, Z. Fate of photosynthetic fixed carbon in light- and shade-adapted colonies of the symbiotic coral *Stylophora pistillata*. *Proc. R. Soc. B Biol. Sci.* **222**, 181–202 (1984).
73. Altieri, A. H., Harrison, S. B., Seemann, J., Collin, R., Diaz, R. J. & Knowlton, N. Tropical dead zones and mass mortalities on coral reefs. *Proc. Natl. Acad. Sci. U. S. A.* **114**, 3660–3665 (2017).
74. Guzmán, H. M. & Guevara, C. Population Structure , Distribution and Abundance of Three Commercial Species of Sea Cucumber ( Echinodermata ) in Panama. *Sci. York* **38**, 230–238 (2002).
75. Guzmán, H. M., Barnes, P. A. G., Lovelock, C. E. & Feller, I. C. A site description of the CARICOMP mangrove, seagrass and coral reef sites in Bocas del Toro, Panama. *Caribb. J. Sci.* **41**, 430–440 (2005).
76. Guzmán, H. M. & Jiménez, C. E. Contamination of coral reefs by heavy metals along the

- Caribbean coast of Central America (Costa Rica and Panama). *Mar. Pollut. Bull.* **24**, 554–561 (1992).
77. Lovelock, C. E., Feller, I. C., McKee, K. L. & Thompson, R. Variation in mangrove forest structure and sediment characteristics in Bocas del Toro, Panama. *Caribb. J. Sci.* **41**, 456–464 (2005).
  78. Rogers, C. S. Responses of coral reefs and reef organisms to sedimentation. *Mar. Ecol. Prog. Ser.* **62**, 185–202 (1990).
  79. Rogers, C. S. The effect of shading on coral reef structure and function. *J. Exp. Mar. Bio. Ecol.* **41**, 269–288 (1979).
  80. Anthony, K. & Larcombe, P. Coral reefs in turbid waters: sediment-induced stresses in corals and likely mechanisms of adaptation. *Proc. 9th Int. Coral Reef Symp.* 239–244 (2000).
  81. Acevedo, R., Morelock, J. & Olivieri, R. A. Modification of coral reef zonation by terrigenous sediment stress. *Palaios* **4**, 92–100 (1989).
  82. Anthony, K. R. N. & Fabricius, K. E. Shifting roles of heterotrophy and autotrophy in coral energetics under varying turbidity. *J. Exp. Mar. Bio. Ecol.* **252**, 221–253 (2000).
  83. Kirk, J. T. O. *Light and Photosynthesis in Aquatic Ecosystems*. (Cambridge University Press, 2010). doi:10.1017/CBO9781139168212
  84. Anthony, K. R. N. & Hoegh-Guldberg, O. Variation in coral photosynthesis, respiration and growth characteristics in contrasting light microhabitats: An analogue to plants in forest gaps and understoreys? *Funct. Ecol.* **17**, 246–259 (2003).
  85. Linsmayer, L. B. & Tresguerres, M. The dynamic oxygen microenvironment of corals: Identification of strombine as the main fermentative end product. (Scripps Institution of Oceanography, 2017).
  86. Ernst, O. & Zor, T. Linearization of the Bradford Protein Assay. *J. Vis. Exp.* 1–6 (2010). doi:10.3791/1918
  87. Delacre, M., Lakens, D. & Leys, C. Why Psychologists should by default use Welch’s t-test instead of Student’s t-test. *Int. Rev. Soc. Psychol.* **30**, 92 (2017).
  88. Nachar, N. The Mann-Whitney U: A Test for Assessing Whether Two Independent Samples Come from the Same Distribution. *Tutor. Quant. Methods Psychol.* **4**, 13–20 (2008).
  89. Ruxton, G. D. The unequal variance t-test is an underused alternative to Student’s t-test and the Mann–Whitney U test. *Behav. Ecol.* **17**, 688–690 (2006).

90. Ludbrook, J. & Dudley, H. Why permutation tests are superior to t and F tests in biomedical research. *Am. Stat.* **52**, 127–132 (1998).
91. Kim, H.-Y. Statistical notes for clinical researchers: assessing normal distribution using skewness and kurtosis. *Restor. Dent. Endod.* **38**, 52 (2013).
92. De Winter, J. C. F. Using the Student's t-Test with Extremely Small Sample Sizes. *Pract. Assessment, Res. Eval.* **18**, (2013).
93. Zimmerman, D. W. & Zumbo, B. D. Rank transformations and the power of the Student t test and Welch t' test for non-normal populations with unequal variances. *Can. J. Exp. Psychol. Can. Psychol. expérimentale* **47**, 523–539 (2007).
94. Ghasemi, A. & Zahediasl, S. Normality tests for statistical analysis: A guide for non-statisticians. *Int. J. Endocrinol. Metab.* **10**, 486–489 (2012).
95. Feng, C., Wang, H., Lu, N., Chen, T., He, H., Lu, Y. & Tu, X. M. Log-transformation and its implications for data analysis. *Shanghai Arch. psychiatry* **26**, 105–109 (2014).
96. Joanest, D. N. & Gill, C. A. Comparing measures of sample skewness and kurtosis. *Stat.* **47**, 183–189 (1998).
97. Wright, D. B. & Herrington, J. A. Problematic standard errors and confidence intervals for skewness and kurtosis. *Behav. Res. Methods* **43**, 8–17 (2011).
98. Groeneveld, R. A. & Meeden, G. Measuring skewness and kurtosis. *Stat.* **33**, 391–399 (1984).
99. Yang, T. H., Lai, N. C., Graham, J. B. & Somero, G. N. Respiratory, Blood, and Heart Enzymatic Adaptations of *Sebastes alascanus* (Scorpaenidae; Teleostei) to the Oxygen Minimum Zone: A Comparative Study. *Biol. Bull.* **183**, 490–499 (1992).
100. Friedman, J. R., Condon, N. E. & Drazen, J. C. Gill surface area and metabolic enzyme activities of demersal fishes associated with the oxygen minimum zone off California. *Limnol. Oceanogr.* **57**, 1701–1710 (2012).
101. Larcombe, P., Ridd, P. V., Prytz, A. & Wilson, B. Factors controlling suspended sediment on inner-shelf coral reefs, Townsville, Australia. *Coral Reefs* **14**, 163–171 (1995).
102. Guppy, M. & Withers, P. Metabolic depression in animals: Physiological perspectives and biochemical generalizations. *Biol. Rev.* **74**, 1–40 (1999).
103. Todgham, A. E. & Hofmann, G. E. Transcriptomic response of sea urchin larvae *Strongylocentrotus purpuratus* to CO<sub>2</sub>-driven seawater acidification. *J. Exp. Biol.* **212**, 2579–2594 (2009).

104. Pörtner, H. O. Ecosystem effects of ocean acidification in times of ocean warming: A physiologist's view. *Mar. Ecol. Prog. Ser.* **373**, 203–217 (2008).
105. Nakamura, M., Ohki, S., Suzuki, A. & Sakai, K. Coral larvae under ocean acidification: Survival, metabolism, and metamorphosis. *PLoS One* **6**, 1–7 (2011).
106. Kaniewska, P., Campbell, P. R., Kline, D. I., Rodriguez-Lanetty, M., Miller, D. J., Dove, S. & Hoegh-Guldberg, O. Major cellular and physiological impacts of ocean acidification on a reef building coral. *PLoS One* **7**, (2012).
107. Jerlov, N. G. Ultra-violet Radiation in the Sea. *Nature* **166**, 111–112 (1950).
108. Morel, A., Gentili, B., Claustre, H., Babin, M., Bricaud, A., Ras, J. & Tièche, F. Optical properties of the 'clearest' natural waters. *Limnol. Oceanogr.* **52**, 217–229 (2007).
109. Fleischmann, E. M. The measurement and penetration of ultraviolet radiation into tropical marine water. *Limnol. Oceanogr.* **34**, 1623–1629 (1989).
110. Shick, M. J., Lesser, M. P. & Jokiel, P. L. Effects of ultraviolet radiation on corals and other coral reef organisms. *Glob. Chang. Biol.* **2**, 527–545 (1996).
111. Lesser, M. P. & Shick, J. M. Effects of irradiance and ultraviolet radiation on photoadaptation in the zooxanthellae of *Aiptasia pallida*: primary production, photoinhibition, and enzymic defenses against oxygen toxicity. *Mar. Biol.* **102**, 243–255 (1989).
112. Banaszak, A. T. & Lesser, M. P. Effects of solar ultraviolet radiation on coral reef organisms. *Photochem. Photobiol. Sci.* **8**, 1276–1294 (2009).
113. Dunlap, W. C. & Shick, J. M. Ultraviolet radiation-absorbing mycosporine-like amino acids in coral reef organisms: A biochemical and environmental perspective. *J. Phycol.* **34**, 418–430 (1998).
114. Gleason, D. F. Ultraviolet Radiation and Coral Communities. in *Ecosystems, Evolution, and Ultraviolet Radiation* 118–149 (2001). doi:10.1007/978-1-4757-3486-7\_5
115. Nakamura, H., Kobayashi, J. & Hirata, Y. Separation of mycosporine-like amino acids in marine organisms using reversed-phase high-performance liquid chromatography. *J. Chromatogr. A* **250**, 113–118 (1982).
116. Dunlap, W. C. & Yamamoto, Y. Small-molecule antioxidants in marine organisms: Antioxidant activity of mycosporine-glycine. *Comp. Biochem. Physiol. -- Part B Biochem.* **112**, 105–114 (1995).
117. Lesser, M. P. Elevated temperatures and ultraviolet radiation cause oxidative stress and



- inhibit photosynthesis in symbiotic dinoflagellates. *Limnol. Oceanogr.* **41**, 271–283 (1996).
118. Gleason, D. F. Differential effects of ultraviolet radiation on green and brown morphs of the Caribbean coral *Porites astreoides*. *Limnol. Oceanogr.* **38**, 1452–1463 (1993).
  119. Kinzie, R. A. & Hunter, T. Effect of light quality on photosynthesis of the reef coral *Montipora verrucosa*. *Mar. Biol.* **94**, 95–109 (1987).
  120. Lesser, M. P., Stochaj, W. R., Tapley, D. W. & Shick, J. M. Bleaching in coral reef anthozoans: effects of irradiance, ultraviolet radiation, and temperature on the activities of protective enzymes against active oxygen. *Coral Reefs* **8**, 225–232 (1990).
  121. Dunne, R. P. & Brown, B. E. Penetration of solar UVB radiation in shallow tropical waters and its potential biological effects on coral reefs; results from the central Indian Ocean and Andaman Sea. *Mar. Ecol. Prog. Ser.* **144**, 109–118 (1996).
  122. Veal, C. J., Holmes, G., Nunez, M., Hoegh-Guldberg, O. & Osborn, J. A comparative study of methods for surface area and three-dimensional shape measurement of coral skeletons. *Limnol. Oceanogr. Methods* **8**, 241–253 (2010).
  123. Jokiel, P. & York Jr, R. Solar ultraviolet photobiology of the reef coral *Pocillopora damicornis* and symbiotic zooxanthellae. *Bull. Mar. Sci.* **32**, 301–315 (1982).
  124. Edmunds, P. J. Zooplanktivory ameliorates the effects of ocean acidification on the reef coral *Porites* spp. *Limnol. Oceanogr.* **56**, 2402–2410 (2011).
  125. Grottoli, A. G., Rodrigues, L. J. & Palardy, J. E. Heterotrophic plasticity and resilience in bleached corals. *Nature* **440**, 1186–1189 (2006).
  126. Goreau, T. F., Goreau, N. I. & Yonge, C. M. Reef corals: Autotrophs or heterotrophs? *Biol. Bull.* **141**, 247–260 (1971).
  127. Fabricius, K. E. Effects of terrestrial runoff on the ecology of corals and coral reefs: Review and synthesis. *Mar. Pollut. Bull.* **50**, 125–146 (2005).
  128. Yeakel, K. L., Andersson, A. J., Bates, N. R., Noyes, T. J., Collins, A. & Garley, R. Shifts in coral reef biogeochemistry and resulting acidification linked to offshore productivity. *Proc. Natl. Acad. Sci.* **112**, 14512–14517 (2015).
  129. Enochs, I. C., Manzello, D. P., Carlton, R., Schopmeyer, S., van Hooidonk, R. & Lirman, D. Effects of light and elevated pCO<sub>2</sub> on the growth and photochemical efficiency of *Acropora cervicornis*. *Coral Reefs* **33**, 477–485 (2014).
  130. Anthony, K. R. N. & Hoegh-Guldberg, O. Kinetics of photoacclimation in corals. *Oecologia* **134**, 23–31 (2003).

131. Hatcher, B. G. Coral reef primary productivity: A beggar's banquet. *Trends in Ecology and Evolution* **3**, 106–111 (1988).
132. Li Gelpi, J., Dordal, A., Montserrat, J., Mazo, A. & Cortes, A. Kinetic studies of the regulation of mitochondrial malate dehydrogenase by citrate. *Biochem. J.* **283**, 289–297 (1992).
133. Dasika, S. K., Vinnakota, K. C. & Beard, D. A. Determination of the catalytic mechanism for itochondrial Malate Dehydrogenase. *Biophys. J.* **108**, 408–419 (2015).
134. Walsh, P. J. Purification and characterization of two allozymic forms of octopine dehydrogenase from California populations of *Metridium senile* - The role of octopine dehydrogenase in the anaerobic metabolism of sea anemones. *J. Comp. Physiol. B* **143**, 213–222 (1981).
135. Levy, O. Diel 'tuning' of coral metabolism: physiological responses to light cues. *J. Exp. Biol.* **209**, 273–283 (2006).
136. Mass, T., Kline, D. I., Roopin, M., Veal, C. J., Cohen, S., Iluz, D. & Levy, O. The spectral quality of light is a key driver of photosynthesis and photoadaptation in *Stylophora pistillata* colonies from different depths in the Red Sea. *J. Exp. Biol.* **213**, 4084–4091 (2010).
137. Salih, A., Larkum, A., Cox, G., Kühl, M. & Hoegh-Guldberg, O. Fluorescent pigments in corals are photoprotective. *Nature* **408**, 850–853 (2000).
138. Kawaguti, S. The effect of green fluorescent pigment on the productivity of the reef corals. *Micronesica* **5**, 313 (1969).
139. Schlichter, D., Fricke, H. W. & Weber, W. Light harvesting by wavelength transformation in a symbiotic coral of the Red Sea twilight zone. *Mar. Biol.* **91**, 403–407 (1986).
140. Hamilton, S. L., Logan, C. A., Fennie, H. W., Sogard, S. M., Barry, J. P., Makukhov, A. D., Tobosa, L. R., Boyer, K., Lovera, C. F. & Bernardi, G. Species-specific responses of juvenile rockfish to elevated pCO<sub>2</sub>: From behavior to genomics. *PLoS One* **12**, 1–23 (2017).
141. Miller, S. L., Chiappone, M., Rutten, L. . & Swanson, D. W. Population status of *Acropora* corals in the Florida Keys. *Proc. 11th Int. Coral Reef Symp.* 775–779 (2008).
142. Hemond, E. M. & Vollmer, S. V. Genetic diversity and connectivity in the threatened staghorn coral (*Acropora cervicornis*) in Florida. *PLoS One* **5**, (2010).
143. Morelock, J., Boulon, K. & Galler, G. Sediment Stress and Coral Reefs. *Proceedings, Energy Ind. ...* (1979).

144. Green, D. H., Edmunds, P. J. & Carpenter, R. C. Increasing relative abundance of *Porites astreoides* on Caribbean reefs mediated by an overall decline in coral cover. *Mar. Ecol. Prog. Ser.* **359**, 1–10 (2008).